Bioorganic Chemistry 86 (2019) 652–664

Contents lists available at ScienceDirect

Bioorganic Chemistry

journal homepage: www.elsevier.com/locate/bioorg

Exploring substituent diversity on pyrrolidine-aryltriazole iminosugars: Structural basis of β-glucocerebrosidase inhibition

Macarena Martínez-Bailén[a], Ana T. Carmona[a,*], Athéna C. Patterson-Orazem[b], Raquel L. Lieberman[b], Daisuke Ide[c], Moemi Kubo[c], Atsushi Kato[c], Inmaculada Robina[a], Antonio J. Moreno-Vargas[a,*]

[a] Department of Organic Chemistry, Faculty of Chemistry, University of Seville, C/Prof. García González, 1, 41012-Seville, Spain
[b] School of Chemistry & Biochemistry, Georgia Institute of Technology, Atlanta 30332-0400, GA, United States
[c] Department of Hospital Pharmacy, University of Toyama, Toyama 930-0194, Japan

ARTICLE INFO

Keywords:
β-glucocerebrosidase inhibitors
Iminosugars
Pyrrolidines
Triazoles
Click chemistry
Protein crystallization
Chaperones

ABSTRACT

The synthesis of a library of pyrrolidine-aryltriazole hybrids through CuAAC between two epimeric dihydroxylated azidomethylpyrrolidines and differently substituted phenylacetylenes is reported. The evaluation of the new compounds as inhibitors of lysosomal β-glucocerebrosidase showed the importance of the substitution pattern of the phenyl moiety in the inhibition. Crystallization and docking studies revealed key interactions of the pyrrolidine motif with aminoacid residues of the catalytic site while the aryltriazole moiety extended along a hydrophobic surface groove. Some of these compounds were able to increase the enzyme activity in Gaucher patient fibroblasts, acting as a new type of chemical chaperone for Gaucher disease.

1. Introduction

Lysosomal storage disorders (LSDs) [1] are inherited metabolic diseases that are characterized by an abnormal accumulation of glycosphingolipids, glycoproteins or mucopolysaccharides in the lysosomes of various cell types resulting from decreased activity of the enzymes responsible for their degradation. Gaucher disease (GD) [2] is the most common LSD and is caused by mutations in the gene encoding lysosomal acid-β-glucosidase (GCase or GBA1). Although more than 200 different mutations have been identified for GBA1 gene, the two most common are N370S and L444P, associated with non-neuronopathic and neuronopathic Gaucher disease, respectively. Additional evidence suggests a relationship between Parkinson disease susceptibility and GBA mutations [3]. The decreased activity of GCase leads to accumulation of glucosylceramide (GlcCer) in several organs including the liver, spleen and brain.

The two main approaches for the treatment of GD are enzyme replacement therapy (ERT), which involves intravenous administration of recombinant GCase, and substrate reduction therapy (SRT), based on inhibiting the biosynthesis of GlcCer, thus limiting its accumulation in the lysosome. However, several limitations related to low blood–brain barrier permeability of the recombinant enzyme and side effects due to inhibiting the synthesis of important gangliosides and cerebrosides in the SRT, require the development of other therapeutic treatments for GD. Pharmacological chaperone therapy (PCT) [4–6] is an emerging strategy based on the use of low molecular weight molecules that bind the misfolded protein and assist proper folding, thus enhancing the activity of the deficient enzyme and controlling substrate accumulation in the lysosome. Some reversible competitive GCase inhibitors at sub-inhibitory concentrations can act as pharmacological chaperones and stabilize mutant GCase, activating the enzyme and avoiding its degradation by endoplasmic reticulum quality control system [7,8]. This approach has been successfully used in the case of Fabry disease, other LSD related with the misfolded α-galactosidase A, with the development of the drug Galafold® (1-deoxygalactonojirimycin, DGJ), recently approved by the European Commission [9]. However, PCT has not yet been successful for the treatment of GD, despite the enormous efforts recently made towards the development of GCase pharmacological chaperones [10–17]. The failure of PCT for GD may be due to low affinity for the enzyme, poor selectivity and limited membrane permeability of inhibitors used [18]. A strategy to circumvent the permeability problem is to design less polar iminosugar inhibitors. Isofagomine (IFG, Fig. 1), a trihydroxylated piperidine with less hydroxylation than other traditional inhibitors such as nojirimycins, increased cellular GCase levels in Gaucher patient tissues, including the brain [19]. However, IFG has exhibited low activity when tested in

* Corresponding authors.
E-mail addresses: anatere@us.es (A.T. Carmona), ajmoreno@us.es (A.J. Moreno-Vargas).

https://doi.org/10.1016/j.bioorg.2019.02.025
Received 9 January 2019; Received in revised form 5 February 2019; Accepted 9 February 2019
Available online 12 February 2019

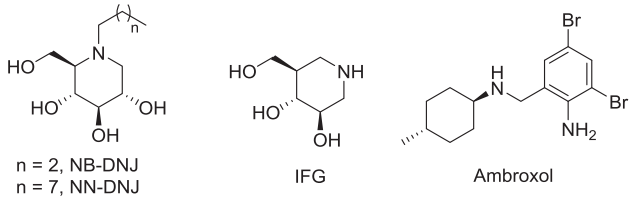

Fig. 1. Structures of representative GCase chaperones.

clinical trials, perhaps because it remains too hydrophilic for facile transport. An alternative to increase the permeability is the incorporation of alkyl substituents on the inhibitors. This strategy was followed in the design of *N*-butyl-deoxynojirimycin (NB-DNJ, Fig. 1) and *N*-nonyl-deoxynojirimycin (NN-DNJ, Fig. 1), making NN-DNJ the first molecule to successfully act as a chemical chaperone *in vivo* for GD [20,21]. Recently, the non-iminosugar drug Ambroxol (Fig. 1) has been reported to act as a chemical chaperone and has shown efficacy in patients with type 1 GD, and is currently under study for the treatment of type 3 GD [22,23]. Although a new family of chaperones that are allosteric binders has been developed [24], most of the chemical chaperones described for GD are iminosugar competitive inhibitors, mainly of the piperidine family [25]. Recently, the first examples of pyrrolidine-based pharmacological chaperones have been reported, all of them bearing a trihydroxylated-iminosugar core [26,27].

We have recently reported the discovery of pyrrolidine-triazole hybrid molecules as selective inhibitors of β-glucosidase (almond) and α-galactosidase (coffee bean) [28]. The most potent inhibitors presented an aryltriazole moiety, with compounds **1–3** proving most active (Fig. 2). Interestingly, these compounds also showed moderate-to-good inhibition towards human lysosomal GCase, making them the first examples of this type of inhibitors with a dihydroxylated-pyrrolidine core. These results, together with previous examples from our research group [29–31] and from others [32–34], support the idea that the incorporation of (hetero)aromatic residues into the iminosugar core augments the potency and selectivity of the inhibitor, probably resulting from additional non-glycone interactions with the enzyme. This approach circumvents the lack of selectivity of most pyrrolidine iminosugars while simultaneously improves their lipophilic character (and thus cellular and ER permeability) crucial for a useful drug.

As an extension of our previous work, we have prepared a small library of new aromatic pyrrolidine-triazole derivatives and here report their glycosidase inhibition properties. We have evaluated the influence in GCase inhibition of modifications at the aryl residue, which we found crucial for inhibitory activity. The influence of structural modifications of the pyrrolidine core, such as the incorporation of a hydroxymethyl substituent and oxidation at C-5, were also analysed (Fig. 3). Besides, we report the co-crystal structure of GCase in complex with one of the new inhibitors, the (2*R*)-3,5-dichlorophenyltriazole (derivative **18**). Finally, the chaperone activity for several of the inhibitors was measured in cells derived from Gaucher patients harbouring the N370S mutant GCase. In sum, our study demonstrates that dihydroxypyrrolidine iminosugars can be considered a new type of pharmacological chaperones for the PCT for Gaucher disease.

2. Results and discussion

2.1. Synthesis of pyrrolidine/pyrrolidinone triazoles

Pyrrolidine triazoles **4–12** were obtained in good to excellent yields through CuAAC reaction between pyrrolidine azides **25** or **26**, recently described by ourselves [28], and alternatively-substituted phenylacetylenes (Scheme 1). Epimeric (2*R*,3*S*,4*R*) pyrrolidine-triazoles **13–21** were prepared from pyrrolidine azide **29**, the synthesis of which was improved compared to one we recently reported [28] (See Supporting Information). Subsequent CuAAC reaction between protected azido pyrrolidine **29** and 4-fluoro(or 4-hydroxy)phenylacetylene and deprotection afforded derivatives **13** and **16**. On the other hand, pyrrolidine-triazoles **17–21** were obtained after CuAAC reaction of unprotected pyrrolidine azide **30** with the corresponding alkynes (Scheme 2). Structures of all new compounds were confirmed by ^{1}H and ^{13}C NMR and mass spectrometry.

To determine whether the introduction of a carbonyl substituent at C-5 of the pyrrolidine ring impacts GCase inhibition, we decided to prepare some pyrrolidinone derivatives. The oxidation of the C-5 position was performed at the azido pyrrolidine stage. Thus, oxidation of azide **25** with $NaIO_4/RuO_2$ in a biphasic system EtOAc/H_2O [35] afforded the corresponding azido pyrrolidinone **31** in 81% yield (Scheme 3). CuAAC reaction with phenylacetylene and 3,5-difluorophenylacetylene followed by acidic deprotection gave triazole derivatives **22** and **23**.

It has been reported that the presence of a terminal CH_2OH group in the iminosugar skeleton has an important role in the inhibition of some glycosidases [36]. Thus, we carried out the synthesis of compound **24** starting from pyrrolidine **32** (Scheme 4). The synthesis of aminomethyl pyrrolidine **32** was accomplished from D-ribose as previously described [37]. Subsequent azido transfer reaction and CuAAC with phenylacetylene yielded pyrrolidine triazole **24** (Scheme 4).

2.2. Glycosidase inhibition studies

The analysis of the inhibition properties of each triazole derivative was carried out against a panel of nine commercial [38] (Supplementary Table S1) and two human glycosidases (GCase and α-galactosidase A). Derivatives **1**, **4–12** were moderate-to-good inhibitors of β-glucosidase from almonds (IC_{50} = 261–8.0 μM, Supplementary Table S1) and of GCase (Table 1) and some interesting correlations between the substitution pattern of the aromatic group and the inhibition potency can be deduced. We observed that *p*-substitution at the phenyl group decreased the inhibitory potency of the derivatives towards GCase relative to the parent non-substituted compound **1**, especially when a CH_2OH is the substituent (compound **5**). The higher inhibitory potency was observed with 3,5-disubstituted derivatives as compared with the *p*-substituted and non-substituted compounds (see inhibitory properties of **12** *vs* **6**, **8** *vs* **7**, **10** *vs* **1**) with derivatives **9–11** the most bioactive compounds (IC_{50} = 1.5–0.83 μM). In general, the presence of halogens in the 3,5-disubstitution pattern of the aromatic core clearly benefits the inhibition (diCl-, diBr-, diCF_3- *vs* diOMe-), increasing the inhibition potency up to 10-fold in the most relevant

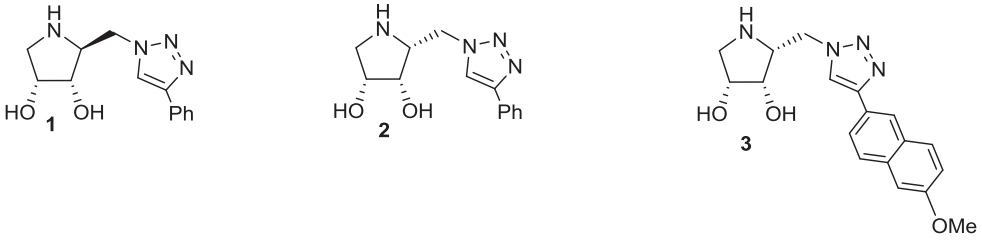

Fig. 2. Pyrrolidine triazoles previously described by Martínez-Bailén et al. [28]

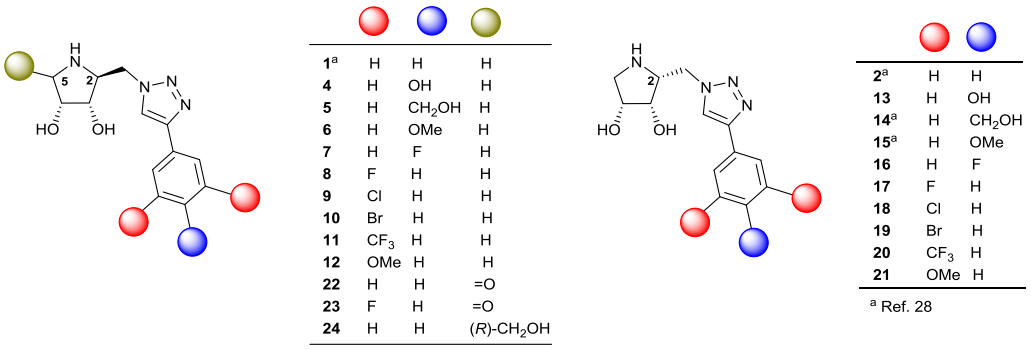

1[a]	H	H	H
4	H	OH	H
5	H	CH_2OH	H
6	H	OMe	H
7	H	F	H
8	F	H	H
9	Cl	H	H
10	Br	H	H
11	CF_3	H	H
12	OMe	H	H
22	H	H	=O
23	F	H	=O
24	H	H	(*R*)-CH_2OH

2[a]	H	H
13	H	OH
14[a]	H	CH_2OH
15[a]	H	OMe
16	H	F
17	F	H
18	Cl	H
19	Br	H
20	CF_3	H
21	OMe	H

[a] Ref. 28

Fig. 3. Pyrrolidine/pyrrolidinone-triazole hybrid molecules.

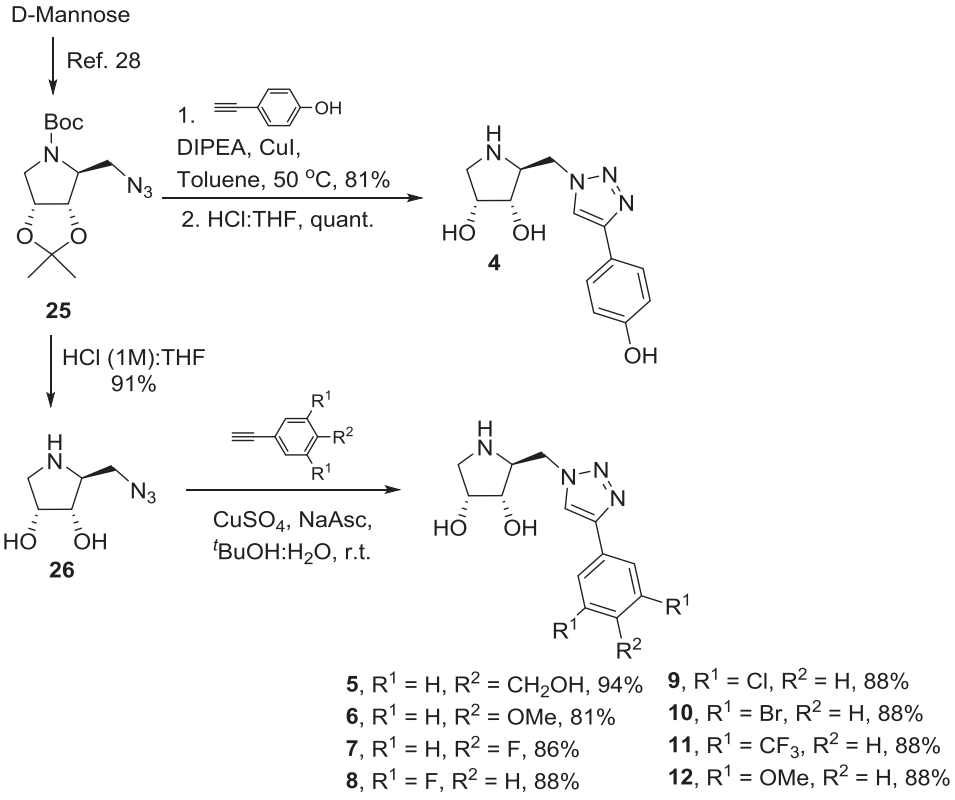

Scheme 1. Synthesis of (2*S*,3*S*,4*R*)-pyrrolidine derivatives **5**–**12**.

example (**10** *vs* **12**, diBr- *vs* diOMe-).

The corresponding C-2 epimers **2**, **13**–**21** were good inhibitors of coffee bean α-galactosidase (IC_{50} = 6.1–37 μM, Supplementary Table S1), but were weak inhibitors of the human α-galactosidase A, although both enzymes belong to the same CAZy (http://www.cazy.org/) [39] family (GH27). Notably, GCase is not able to discriminate between pyrrolidine epimers, as expected based on our observations for parent epimers **1** and **2** [28]. There is high similarity between the activities of each C-2 epimeric pyrrolidine pairs towards this enzyme, whose activity seems to be governed by the aromatic moiety. To illustrate this correlation, a graphic representation of the pIC_{50} (-log IC_{50}) for each pair of epimeric inhibitors has been included (Fig. 4).

On the other hand, structural modifications at C-5 of the pyrrolidine core were detrimental for the inhibition of GCase. Oxidation at C-5 of the pyrrolidine core improved the potency as inhibitor of β-glucosidase from almonds of the resulting lactams **22** and **23** (IC_{50} = 1.8–2.0 μM, see Table S1), but this modification abolished the inhibition of the human β-glucosidase. The introduction of a hydroxymethyl substituent at C-5 (compound **24**) elicited a similar effect upon the inhibition of the human enzyme; moreover, in this case, the inhibition of the plant enzyme was not improved (IC_{50} = 163 μM for **24** *vs* IC_{50} = 8.0 μM for **1**, Table S1).

2.3. Crystal structure of pyrrolidine-triazole *18*:GCase

The overall structure of GCase in complex with pyrrolidine-triazole **18**, which was solved to 2.1 Å resolution (Table S2, Supporting Information, PDB code 6MOZ), closely resembles previously published structures of GCase [40]. In this structure, which contains two monomers in the asymmetric unit, one monomer has glycerol bound in the active site, and the other has **18** bound (Fig. 5a). The catalytic site is nested within the triosephosphate isomerase (TIM) barrel domain. The glycerol-bound monomer is nearly identical to previously-published structures of apo (2NT1) and glycerol-bound (2NSX) with root mean squared deviations (r.m.s.d) less than 0.55 Å. Loop 1 (residues 311 to 319) and 2 (residues 342 to 354) are folded over the catalytic site, in the previously-described "closed lid" conformation (Fig. 5b). The **18**-bound monomer is similar (r.m.s.d. 0.55 Å) to GCase bound to isofagomine (IFG, 2NSX) or covalently linked to a larger inhibitor compound (JZ-5029, 5LVX) [41], with the anticipated conformational

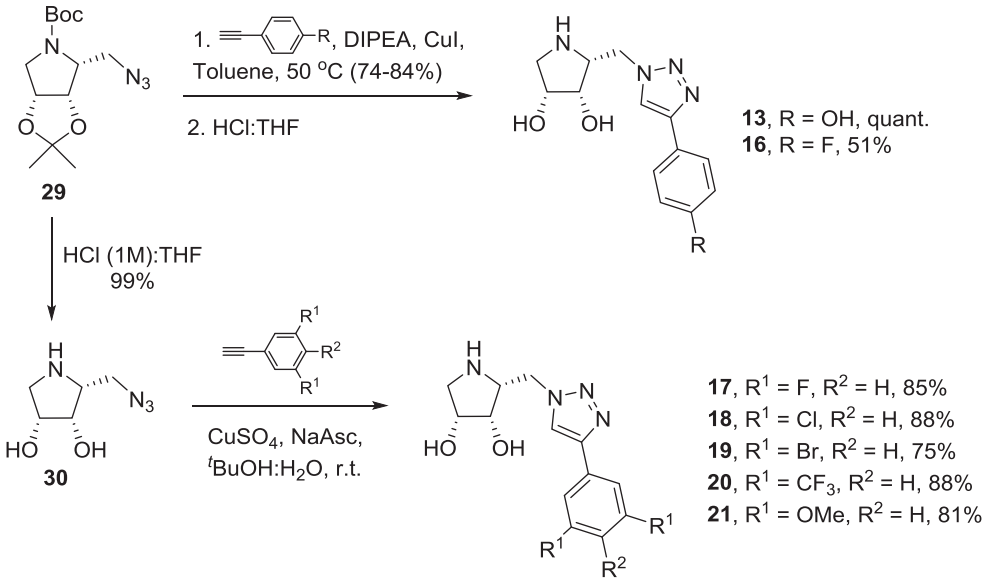

Scheme 2. Synthesis of (2*R*,3*S*,4*R*)-pyrrolidine derivatives **13**, **16–21**.

changes of loops 1 and 2 observed upon inhibitor binding (Fig. 5c). The α-helical arrangement of loop 1 pulls it away from the catalytic site, exposing hydrophobic residues and allowing Tyr 313 to swivel towards the catalytic site, whereas loop 2 shifts to thrust Ser 345 towards the binding pocket (Fig. 6).

GCase binds **18** with the catalytic glutamates 235 and 340 anchoring the nitrogen of the pyrrolidine with hydrogen-bonding interactions. The 4′-hydroxyl is oriented towards a hydrophilic pocket, and 3′-hydroxyl forms H-bonds with Asp 127 and Asn 396 (Fig. 6a). The remainder of the inhibitor extends along a hydrophobic surface groove. The triazole moiety participates in a water-mediated interaction with Ser 345, and the side chain of Tyr 313 appears to participate in a π-π stacking interaction (4.4 Å). Thus, the triazole moiety contributes energetically to inhibitor binding. The phenyl moiety is observed only weakly in the structure, as measured by elevated thermal (B-) factors (Fig. 5a) and weaker electron density (Fig. 6a), suggesting this portion of the molecule is either sampling numerous conformations or is only weakly interacting with GCase. Since our SAR study suggests that substitutions to the phenyl group, and indeed the presence of the phenyl group, affect binding, this portion is likely contributing binding energy despite being weakly resolved in the structure. This portion of the molecule is also likely playing a role in facilitating transport into the cell and the endoplasmic reticulum. Binding of glycerol to GCase involves similar hydrogen-bonding patterns with catalytic glutamates 235 and 340, Asp 127, and tryptophans 179 and 381. The interaction with Asn 396 is exchanged for Asn 234. As compared to the inhibitor-bound conformation, Tyr 313 is flipped away from the catalytic site. While the specific orientation of the glycerol varies slightly from those found in 2NSX, the interacting residues are largely identical.

To assess the binding mode of **10** and **11**, which have different stereochemistry than **18** and for which determination of cocrystal structures was unsuccessful, **11** was docked into the inhibitor-binding monomer of our crystal structure using an AutoDock-based online server [42]. The *in silico* pyrrolidine pose closely resembles that of **18**, but the interaction between the 3′-hydroxyl and Asp 127 is exchanged for an interaction between the 4′-hydroxyl and Trp 179. The triazole and phenyl moieties are directed along the hydrophobic pocket at a slightly different angle relative to **18**. Small changes in loop conformation may accommodate specific interactions with the triazole and phenyl groups across the inhibitor family. Overall, the ability of the hydrophobic pocket of GCase to bind either epimer of the inhibitor supports conformational plasticity of the active site to accommodate a variety of different molecules using weak interactions.

2.4. Chaperone studies

The chaperone activity for the three most potent inhibitors (**10**, **11** and **18**) was evaluated *in vitro* in fibroblasts from Gaucher patients with the N370S mutation. Cells were cultured in the presence of the inhibitors (10–100 μM) for 6 days, and the intracellular enzyme activities were determined with 4-methylumbelliferyl β-glucopyranoside as substrate (Fig. 7). Isofagomine (10–100 μM), a well-studied pharmacological chaperone able to increase the activity of N370S mutant acid β-glucosidase in Gaucher fibroblasts [43] was used as a positive control.

Relative to the non-treated control, compound **11** displayed 1.9 to 2.1-fold enhancement of intracellular β-glucocerebrosidase activity in N370S fibroblasts, comparable to that obtained with isofagomine at the same concentration (10 μM), Increasing the dose up to 100 μM, the result is also comparable between both compounds. This result could be attributed to increased permeability of **11** over isofagomine, which allows the former to more efficiently penetrate the cells, reaching the mutant enzyme more efficiently than isofagomine. Nevertheless, another hypothesis could not be discarded. A stronger binder, as isofagomine, may stabilize the protein to a greater extent, but at the same time it might also inhibit the enzyme more strongly. For a weaker binder (weaker inhibitor), as compound **11**, the inhibition of the

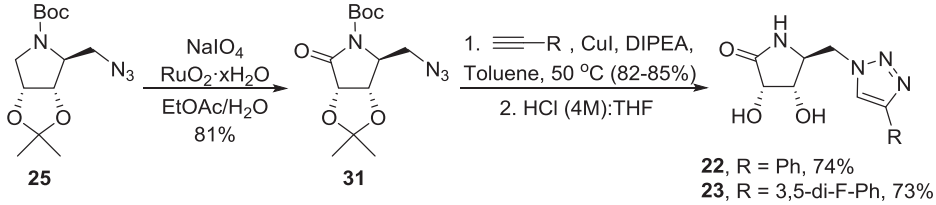

Scheme 3. Synthesis of (3*S*,4*S*,5*S*)-pyrrolidinone derivatives **22–23**.

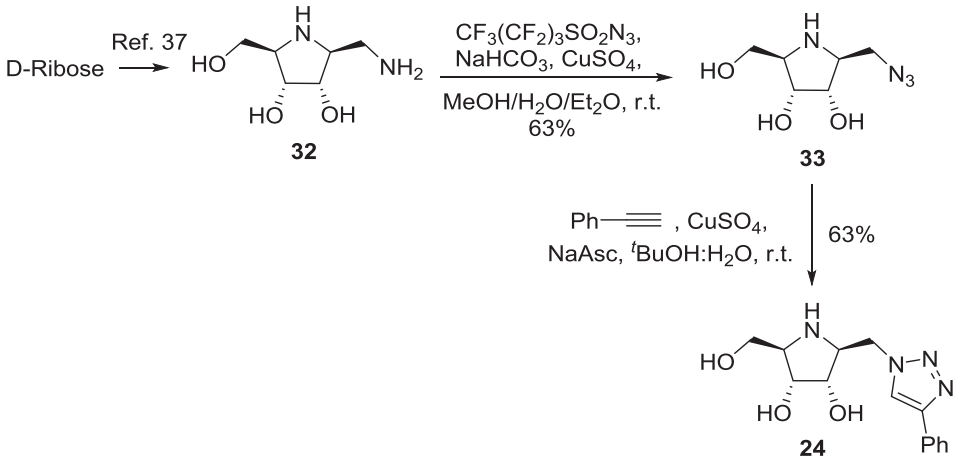

Scheme 4. Synthesis of (2*S*,3*S*,4*R*,5*R*) pyrrolidine derivative **24**.

enzyme is less pronounced and, therefore, the balance chaperone/inhibition of both compounds would be similar. The behavior of dibrominated and dichlorinated derivatives **10** and **18** was very similar to that of **11** and isofagomine, but elicited a slightly smaller enhancement of the enzyme activity at 10 μM. However, in the case of **10**, the enhancement did not increase with the dose. No chaperone effect was detected at lower concentrations (1 and 5 μM) of compounds **10**, **11** and **18**.

In order to confirm that the complex of our compounds with the mutant GCase enhances GCase trafficking from the ER to the lysosome, immunolabeling experiments were performed using N370S Gaucher fibroblasts. Wild type fibroblasts were used as reference. In these assays, if the compound improves GCase trafficking, the amount of the enzyme in the lysosome increases and an enhanced colocalization between GCase and the lysosomal marker (LAMP-1) is observed. Compound **18**, which showed a chaperone activity close to **11** and was crystallized in complex with GCase, was selected for this experiment. Gaucher patient fibroblasts were incubated in the presence of 100 μM **18** for 5 days. The subcellular location of GCase was then determined by double immunofluorescence analysis (Fig. 8). Compared with non-treated cells, the GCase staining pattern of **18**-treated cells showed some overlap with that for lysosomal marker LAMP-1, indicating the presence of GCase in the lysosome what could be due to a slight improvement of the subcellular trafficking and distribution of the mutant enzyme.

3. Conclusions

The inhibition of GCase by epimeric dihydroxypyrrolidine-aryltriazole hybrids was significantly influenced by the substitution pattern of the aromatic moiety, with the 3,5-disubstitution the most effective. Although GCase did not discriminate between C-2 pyrrolidine epimers, the enzyme was highly sensitive to structural modifications at C-5 (oxidation and insertion of CH_2OH), which were detrimental for

Table 1
IC_{50} values (in μM) for the inhibition of β-glucocerebrosidase (GCase, human lysosome) and α-galactosidase A (α-Gal A, human lysosome) by aromatic pyrrolidine-triazole hybrids (**1**, **4–12** and **2**, **13–21**).

	GCase (human lysosome)	α-Gal A (human lysosome)		GCase (human lysosome)	α-Gal A (human lysosome)
1, $R^1 = R^2 = H$	11[a]	NI[a]	**2**, $R^1 = R^2 = H$	28[a]	171[a]
4, $R^1 = H$, $R^2 = OH$	27	NI	**13**, $R^1 = H$, $R^2 = OH$	34	251
5, $R^1 = H$, $R^2 = CH_2OH$	102	NI	**14**, $R^1 = H$, $R^2 = CH_2OH$	187[a]	159[a]
6, $R^1 = H$, $R^2 = OMe$	39	NI	**15**, $R^1 = H$, $R^2 = OMe$	31[a]	185[a]
7, $R^1 = H$, $R^2 = F$	23	NI	**16**, $R^1 = H$, $R^2 = F$	24	388
8, $R^1 = F$, $R^2 = H$	3.8	NI	**17**, $R^1 = F$, $R^2 = H$	5.7	618
9, $R^1 = Cl$, $R^2 = H$	1.5	NI	**18**, $R^1 = Cl$, $R^2 = H$	1.3	360
10, $R^1 = Br$, $R^2 = H$	0.83	NI	**19**, $R^1 = Br$, $R^2 = H$	1.4	387
11, $R^1 = CF_3$, $R^2 = H$	0.95	NI	**20**, $R^1 = CF_3$, $R^2 = H$	1.6	NI
12, $R^1 = OMe$, $R^2 = H$	8.3	NI	**21**, $R^1 = OMe$, $R^2 = H$	7.3	352

NI: no inhibition detected (or less than 50%) at 1 mM of inhibitor.
[a] Data from Ref. [28].

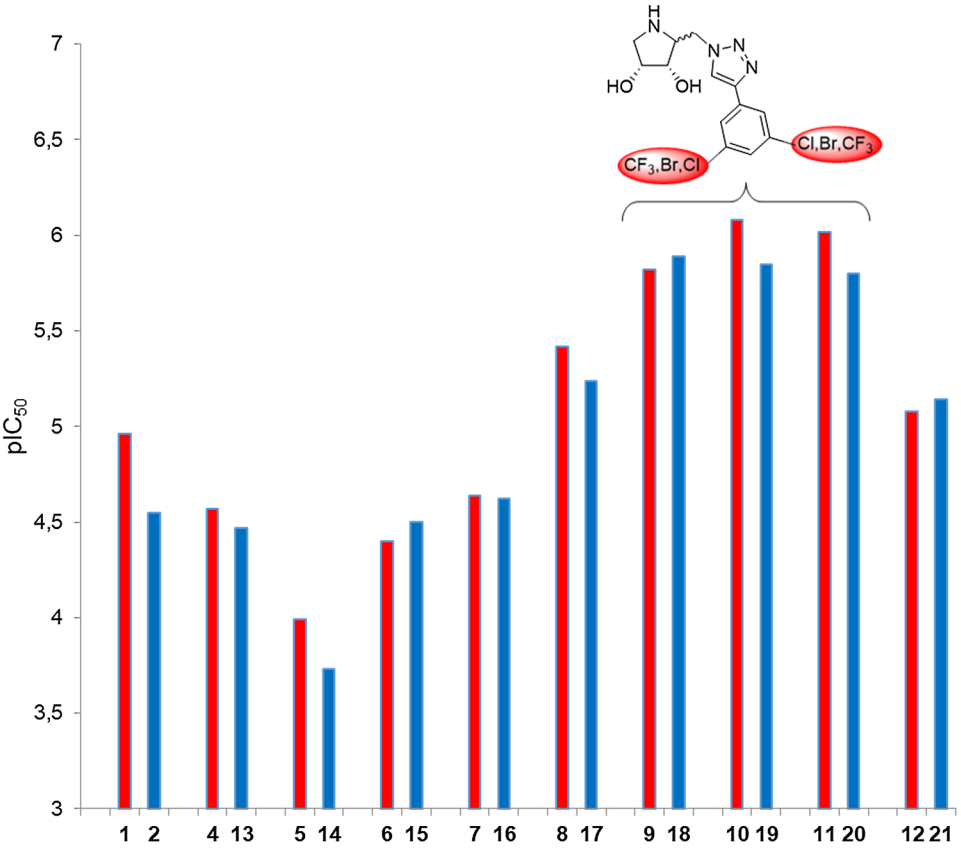

Fig. 4. Representation of pIC_{50} ($-\log IC_{50}$) values for the inhibition of β-glucocerebrosidase (human lysosome) by each pair of epimeric inhibitors (2*S*-pyrrolidine-triazoles in blue, 2*R*-pyrrolidine-triazoles in red). (For interpretation of the references to colour in this figure legend, the reader is referred to the web version of this article.)

enzyme inhibition. Selected inhibitors were capable of increasing the *in vitro* activity of GCase in Gaucher patient fibroblasts. The co-crystal structure of **18** and GCase showed key binding interactions between the pyrrolidine core and the catalytic site residues. Besides, docking experiments suggested the accommodation of the aryltriazole moiety in the hydrophobic pocket of the enzyme. The low degree of hydroxylation of the new compounds and the presence of a lipophilic aromatic residue is remarkable and could improve the drug-like properties of these compounds, including cell-membrane penetration. Dihydroxypyrrolidine-aryltriazoles therefore represent a new family of chemical chaperones of interest for the search of efficient PCTs for Gaucher disease.

4. Methods

4.1. Chemistry

4.1.1. General methods

Optical rotations were measured in a 1.0 cm or 1.0 dm tube with a Jasco P-2000 spectropolarimeter. Infrared spectra were recorded with a Jasco FTIR-410 spectrophotometer. ^{1}H and ^{13}C NMR spectra were recorded with a Bruker AMX300, AV300 for solutions in $CDCl_3$, DMSO-d_6 and CD_3OD. δ are given in ppm and *J* in Hz. *J* are assigned and not repeated. All the assignments were confirmed by COSY and HSQC experiments. High resolution mass spectra were recorded on a Q-Exactive spectrometer. NMR and mass spectra were registered in CITIUS (University of Seville). TLC was performed on silica gel 60 F_{254} (Merck), with detection by UV light charring with *p*-anisaldehyde, $KMnO_4$, ninhydrin or with Pancaldi reagent [$(NH_4)_6MoO_4$, $Ce(SO_4)_2$, H_2SO_4, H_2O]. Silica gel 60 (Merck, 40–60 and 63–200 μm) was used for preparative chromatography.

CuAAC-Procedure 1: To a solution of the unprotected pyrrolidine-azide in ^{t}BuOH:H_2O 2:1 (25–30 mM), the corresponding alkyne (1.2 eq), sodium ascorbate (0.11–0.22 eq) and $CuSO_4$ (0.034–0.068 eq) were added and the solution was stirred at r.t. for 15–24 h. The solvent was evaporated, and the resulting residue was purified by chromatography column on silica gel.

CuAAC-Procedure 2: To a solution of the protected pyrrolidine-azide in toluene:DMF (3:1) or toluene, the corresponding alkyne (3.0–7.0 eq), DIPEA (3.8 eq) and CuI (0.3–0.6 eq) were added and the solution was stirred at 50 °C for 24–60 h. The solvent was evaporated, and the resulting residue was dissolved in EtOAc and aq. sat. soln. of $NaHCO_3$ was added. The aqueous phase was extracted with EtOAc (x2) and the organic layers were dried over Na_2SO_4, filtered and evaporated. The resulting residue was purified by chromatography column on silica gel.

General procedure for acidic deprotection: A solution of the protected (pyrrolidin-2-yl)triazole derivative in HCl (4 M):THF 1:1 was stirred at r.t. for 3 h and evaporated.

(2*S*,3*S*,4*R*)-2-[(4-(4-Hydroxyphenyl)-1*H*-1,2,3-triazol-1-yl)methyl]-pyrrolidine-3,4-diol hydrochloride (4): CuAAC (*Procedure 2*) using **25** [28] (91 mg, 0.31 mmol) and 4-ethynylphenol [44] followed by chromatography purification (EtOAc:cyclohexane 1:1) yielded (2*S*,3*S*,4*R*)-*N*-*tert*-butoxycarbonyl-2-[(4-(4-hydroxyphenyl)-1*H*-1,2,3-triazol-1-yl)methyl]-3,4-*O*-isopropylidene-pyrrolidine-3,4-diol (104 mg, 0.250 mmol, 81%) as a pale yellow solid. Subsequent acidic deprotection (87 mg, 0.21 mmol), yielded **4** (74 mg, 0.21 mmol, quant.) as a purple solid. $[\alpha]_D^{25}$ – 45.3 (*c* 0.69, MeOH). IR (ν cm^{-1}) 3129 (OH, NH), 2901, 1616, 1515, 1229, 833, 676. ^{1}H NMR (300 MHz, CD_3OD, δ ppm, *J* Hz) *δ* 8.53 (s, 1H, H-5″), 7.70–7.65 (m, 2H, H-aromat.), 6.92–6.87 (m, 2H, H-aromat.), 5.01–4.99 (m, 2H, H-1′), 4.30 (ap. t, 1H, H-4), 4.20 (dd, 1H, $J_{3,2}$ = 9.6, $J_{3,4}$ = 3.8, H-3), 4.11–4.03 (m, 1H, H-2), 3.59 (dd, 1H, $^2J_{5a,5b}$ = 12.7, $J_{5a,4}$ = 3.7, H-5a), 3.35–3.32 (m, 1H, H-5b). ^{13}C NMR (75.4 MHz, CD_3OD, δ ppm, *J* Hz) *δ* 160.0 (Cq aromat.), 148.4 (C-4″), 128.7 (C aromat.), 123.4 (C-5″), 120.6 (Cq aromat.), 117.0 (C aromat.), 74.8 (C-3), 70.3 (C-4), 60.8 (C-2), 51.7 (C-5), 51.1 (C-1′). HRESIMS *m/z* found 277.1297, calc. for $C_{13}H_{17}N_4O_3$ $[M]^+$: 277.1295.

(2*S*,3*S*,4*R*)-2-[(4-(4-Hydroxymethylphenyl)-1*H*-1,2,3-triazol-1-

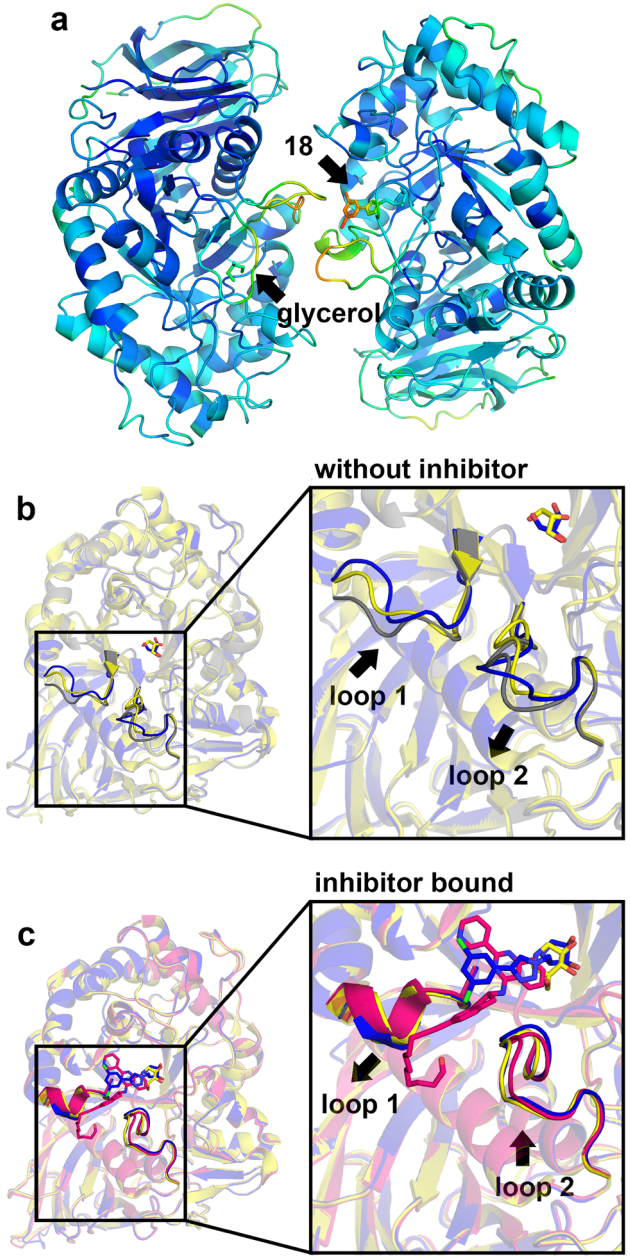

Fig. 5. Overall structure of GCase in complex with 18. (a) Overview of asymmetric unit demonstrating interface between glycerol- and **18**- bound GCase, colored by B-factor (blue, low, to red, high). (b) Structure of glycerol-bound monomer (blue, 6MOZ) superimposed with previously published apo (grey, 2NT1) and glycerol-bound (yellow, 2NSX) structures. (c) Structure of **18**-bound GCase monomer (blue, 6MOZ) aligned with previously published isofagomine-bound (yellow, 2NSX) and JZ-5029-bound (magenta, 5LVX) structures. Inserts are enlarged to clarify characteristic shifts in loops 1 and 2. (For interpretation of the references to colour in this figure legend, the reader is referred to the web version of this article.)

yl)methyl] -pyrrolidine-3,4-diol (5): CuAAC (*Procedure 1*) using **26** [28] (26 mg, 0.16 mmol) and (4-ethynylphenyl)methanol [45] followed by chromatography purification (CH_2Cl_2:MeOH 5:1:0.1→3:1.3:0.5) yielded **5** (42 mg, 0.15 mmol, 94%) as a white solid. $[\alpha]_D^{26}$ – 26.9 (*c* 0.62, DMSO). IR (ν cm^{-1}) 3277, 3172 (OH, NH), 2895, 1498, 1342, 1226, 1052, 815. ^{1}H NMR (300 MHz, DMSO-d_6, δ ppm, *J* Hz) δ 8.48 (s, 1H, H-5″), 7.80 (d, 2H, $J_{H,H}$ = 8.2, H-aromat.), 7.38 (d, 2H, H-aromat.), 5.20 (br. s, 1H, –CH_2OH), 4.76 (br. s, 1H, OH-3), 4.56–4.47 (m, 4H, OH-4, –CH_2OH, H-1′a), 4.28 (dd, 1H, $^2J_{1'b,1'a}$ = 13.7, $J_{1'b,2}$ = 7.9, H-1′b), 3.86–3.81 (m, 1H, H-4), 3.59 (ap. t, 1H, H-3), 3.43–3.17 (m, 2H, NH, H-2), 2.94 (dd, 1H, $^2J_{5a,5b}$ = 11.2, $J_{5a,4}$ = 5.0, H-5a), 2.68 (dd, 1H, $J_{5b,4}$ = 3.5, H-5b). ^{13}C NMR (75.4 MHz, DMSO-d_6, δ ppm) δ 146.0 (C-4″), 142.1 (Cq aromat.), 129.4 (Cq aromat.), 126.9 (C aromat.), 124.9 (C aromat.), 121.7 (C-5″), 74.6 (C-3), 70.8 (C-4), 62.7 (–CH_2OH), 61.8 (C-2), 53.3 (C-1′), 51.4 (C-5). HRESIMS *m/z* found 291.1454, calc. for $C_{14}H_{19}N_4O_3$ $[M + H]^+$: 291.1452.

(2*S*,3*S*,4*R*)-2- [(4-(4-Methoxyphenyl)-1*H*-1,2,3-triazol-1-yl)methyl] -pyrrolidine-3,4-diol (6): CuAAC (*Procedure 1*) using **26** [28] (25 mg, 0.16 mmol) and 1-ethynyl-4-methoxybenzene, followed by chromatography purification (CH_2Cl_2:MeOH:NH_4OH 6:1:0.1) yielded **6** (39 mg, 0.13 mmol, 81%) as a white solid. $[\alpha]_D^{25}$ – 27.7 (*c* 0.60, MeOH). IR (ν cm^{-1}) 3245, 3048 (OH, NH), 2912, 1616, 1560, 1251, 1031, 833, 637. ^{1}H NMR (300 MHz, CD_3OD, δ ppm, *J* Hz) δ 8.24 (s, 1H, H-5″), 7.76–7.71 (m, 2H, H-aromat.), 7.02–6.97 (m, 2H, H-aromat.), 4.67 (dd, 1H, $^2J_{1'a,1'b}$ = 14.0, $J_{1'a,2}$ = 4.1, H-1′a), 4.45 (dd, 1H, $J_{1'b,2}$ = 8.1, H-1′b), 4.04 (td, 1H, $J_{4,3}$ = $J_{4,5a}$ = 4.9, $J_{4,5b}$ = 2.9, H-4), 3.83 (s, 3H, –OCH_3), 3.77 (dd, 1H, $J_{3,2}$ = 7.7, H-3), 3.51 (td, 1H, H-2), 3.15 (dd, 1H, $^2J_{5a,5b}$ = 12.1, H-5a), 2.87 (dd, 1H, H-5b). ^{13}C NMR (75.4 MHz, CD_3OD, δ ppm) δ 161.3 (Cq aromat.), 148.8 (C-4″), 128.0 (C aromat.), 124.3 (Cq aromat.), 122.1 (C-5″), 115.4 (C aromat.), 76.2 (C-3), 72.3 (C-4), 62.7 (C-2), 55.8 (–OCH_3), 54.1 (C-1′), 52.3 (C-5). HRESIMS *m/z* found 291.1453, calc. for $C_{14}H_{19}N_4O_3$ $[M + H]^+$: 291.1452.

(2*S*,3*S*,4*R*)-2- [(4-(4-Fluorophenyl)-1*H*-1,2,3-triazol-1-yl)methyl] -pyrrolidine-3,4-diol (7): CuAAC (*Procedure 1*) using **26** [28] (22 mg, 0.14 mmol) and 1-ethynyl-4-fluorobenzene, followed by chromatography purification (CH_2Cl_2:MeOH:NH_4OH 6:1:0.1→5:1:0.1) yielded **7** (34 mg, 0.12 mmol, 86%) as a white solid. $[\alpha]_D^{28}$ – 36.1 (*c* 0.52, MeOH). IR (ν cm^{-1}) 3258, 3098 (OH, NH), 2926, 1611, 1560, 1497, 1232, 1110, 834, 669. ^{1}H NMR (300 MHz, CD_3OD, δ ppm, *J* Hz) δ 8.33 (s, 1H, H-5″), 7.86–7.80 (m, 2H, H-aromat.), 7.20–7.13 (m, 2H, H-aromat.), 4.68 (dd, 1H, $^2J_{1'a,1'b}$ = 14.0, $J_{1'a,2}$ = 4.1, H-1′a), 4.46 (dd, 1H, $J_{1'b,2}$ = 8.1, H-1′b), 4.05 (td, 1H, $J_{4,3}$ = $J_{4,5a}$ = 4.8, $J_{4,5b}$ = 2.9, H-4), 3.78 (dd, 1H, $J_{3,2}$ = 7.8, H-3), 3.51 (td, 1H, H-2), 3.15 (dd, 1H, $^2J_{5a,5b}$ = 12.1, H-5a), 2.87 (dd, 1H, H-5b). ^{13}C NMR (75.4 MHz, CD_3OD, δ ppm, *J* Hz) δ 164.1 (d, $^1J_{C,F}$ = 245.7, C-4‴), 147.9 (C-4″), 128.6 (d,$^3J_{C,F}$ = 8.2, C-2‴, C-6‴), 128.2 (d, $^4J_{C,F}$ = 3.3, C-1‴), 122.9 (C-5″), 116.8 (d, $^2J_{C,F}$ = 22.0, C-3‴, C-5‴), 76.2 (C-3), 72.3 (C-4), 62.7 (C-2), 54.1 (C-1′), 52.3 (C-5). HRESIMS *m/z* found 279.1253, calc. for $C_{13}H_{16}FN_4O_2$ $[M + H]^+$: 279.1252.

(2*S*,3*S*,4*R*)-2- [(4-(3,5-Difluorophenyl)-1*H*-1,2,3-triazol-1-yl) methyl] -pyrrolidine-3,4-diol (8): CuAAC (*Procedure 1*) using **26** [28] (26 mg, 0.16 mmol) and 1-ethynyl-3,5-difluorobenzene, followed by chromatography purification (CH_2Cl_2:MeOH:NH_4OH 6:1:0.1→5:1:0.1) yielded **8** (41 mg, 0.14 mmol, 88%) as a white solid. $[\alpha]_D^{23}$ – 34.1 (*c* 0.63, MeOH). IR (ν cm^{-1}) 3450, 3288 (OH, NH), 2917, 1629, 1592, 1431, 1226, 1119, 847, 675. ^{1}H NMR (300 MHz, CD_3OD, δ ppm, *J* Hz) δ 8.44 (s, 1H, H-5″), 7.48–7.40 (m, 2H, H-2‴, H-6‴), 6.92 (tt, 1H, $J_{H,F}$ = 9.1, $^4J_{H,H}$ = 2.4, H-4‴), 4.68 (dd, 1H, $^2J_{1'a,1'b}$ = 14.0, $J_{1'a,2}$ = 4.2, H-1′a), 4.47 (dd, 1H, $J_{1'b,2}$ = 8.1, H-1′b), 4.05 (td, 1H, $J_{4,3}$ = $J_{4,5a}$ = 4.9, $J_{4,5b}$ = 2.9, H-4), 3.78 (dd, 1H, $J_{3,2}$ = 7.8, H-3), 3.51 (td, 1H, H-2), 3.14 (dd, 1H, $^2J_{5a,5b}$ = 12.1, H-5a), 2.87 (dd, 1H, H-5b). ^{13}C NMR (75.4 MHz, CD_3OD, δ ppm, *J* Hz) δ 165.0 (dd, $^1J_{C,F}$ = 246.6, $^3J_{C,F}$ = 13.2, C-3‴, C-5‴), 146.7 (t, $^4J_{C,F}$ = 3.2, C-4″), 135.4 (t, $^3J_{C,F}$ = 10.5, C-1‴), 124.1 (C-5″), 109.6–109.2 (m, C-2‴, C-6‴), 104.0 (t, $^2J_{C,F}$ = 26.0, C-4‴), 76.3 (C-3), 72.3 (C-4), 62.7 (C-2), 54.2 (C-1′), 52.4 (C-5). HRESIMS *m/z* found 297.1156, calc. for $C_{13}H_{15}F_2N_4O_2$ $[M + H]^+$: 297.1158.

(2*S*,3*S*,4*R*)-2- [(4-(3,5-Dichlorophenyl)-1*H*-1,2,3-triazol-1-yl) methyl] -pyrrolidine-3,4-diol (9): CuAAC (*Procedure 1*) using **26** [28] (25 mg, 0.16 mmol) and 1,3-dichloro-5-ethynylbenzene [46] followed by chromatography purification (CH_2Cl_2:MeOH:NH_4OH 6:1:0.1) yielded **9** (46 mg, 0.14 mmol, 88%) as a white solid. $[\alpha]_D^{25}$ – 26.2 (*c* 0.57, MeOH). IR (ν cm^{-1}) 3267, 3121 (OH, NH), 2923, 1602, 1567, 1409, 1116, 798, 675. ^{1}H NMR (300 MHz, CD_3OD, δ ppm, *J* Hz) δ 8.45 (s, 1H, H-5″), 7.79 (d, 2H, $^4J_{H,H}$ = 1.9, H-2‴, H-6‴), 7.39 (t, 1H, H-4‴), 4.68 (dd, 1H, $^2J_{1'a,1'b}$ = 14.0, $J_{1'a,2}$ = 4.2, H-1′a), 4.46 (dd, 1H, $J_{1'b,2}$ = 8.1,

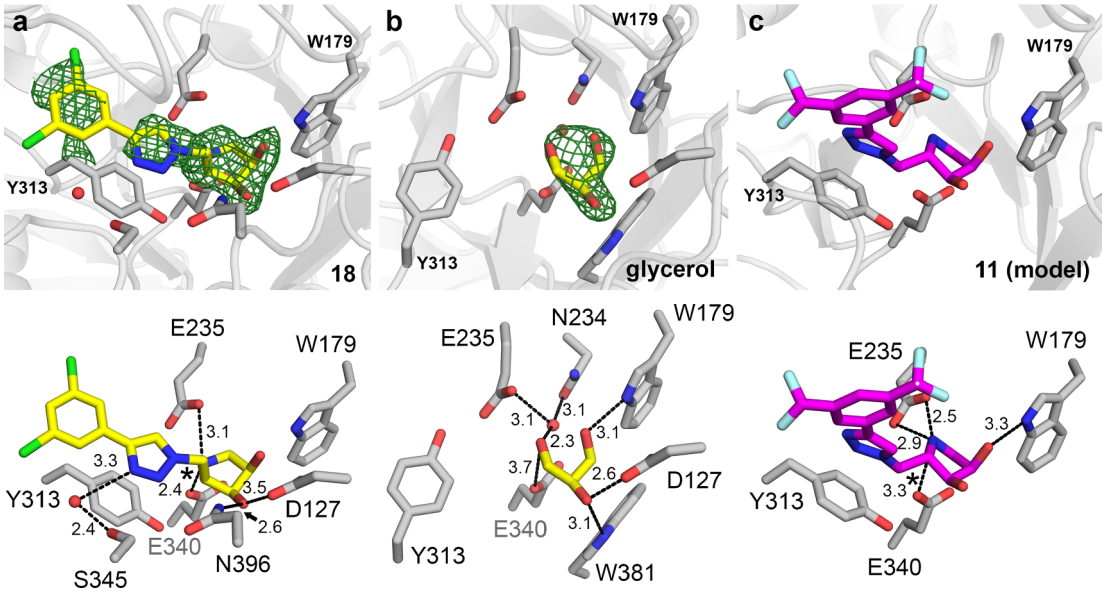

Fig. 6. Binding interactions of (a) pyrrolidine-triazole 18, (b) glycerol and (c) 11 in GCase active site. Binding pose for **11** was computationally docked. Above: green mesh represents Fourier difference maps Fo-Fc, calculated from the refined protein model prior to addition of ligands and contoured at 3σ. The active sites are oriented relative to Tyr 313 and Trp 179. Below: individual interacting residues are labeled including hydrogen bond interactions (dashed lines, Å). The key chiral carbon center which distinguishes **11** (2*S*) and **18** (2*R*) is marked with an asterisk. (For interpretation of the references to colour in this figure legend, the reader is referred to the web version of this article.)

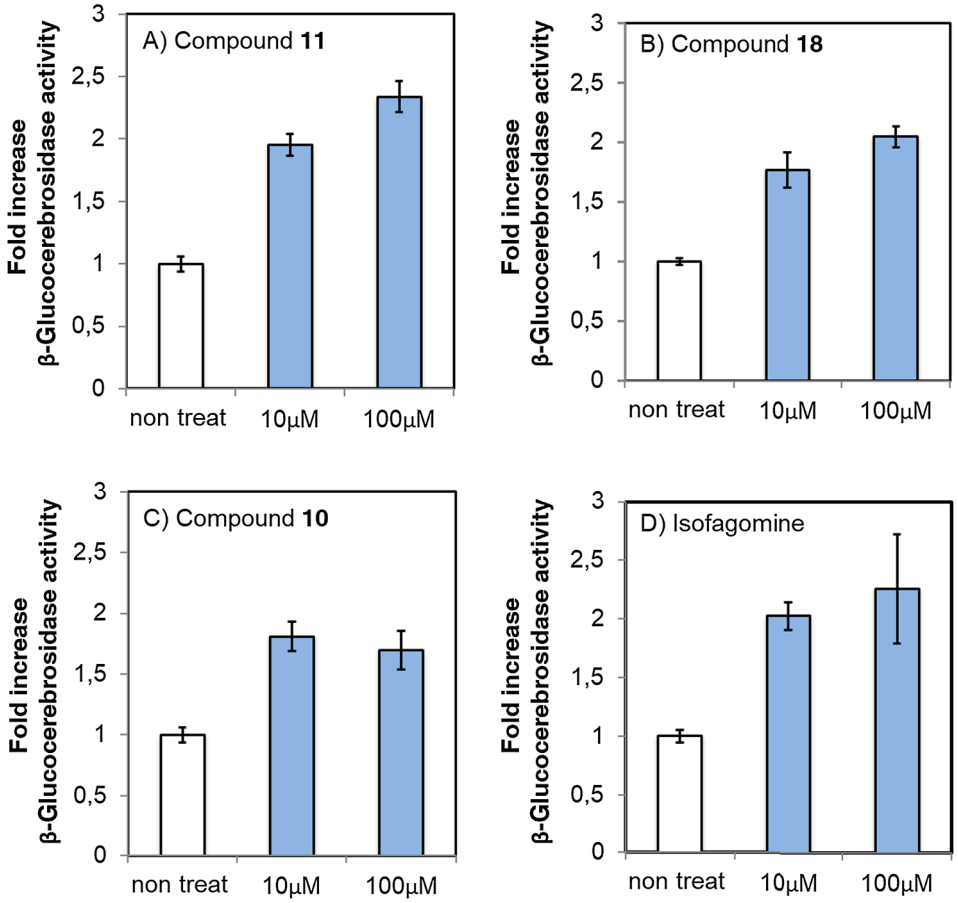

Fig. 7. Effect of pyrrolidine-triazole hybrids (**10**, **11**, **18** and isofagomine) on N370S GCase in Gaucher cells treated with increasing concentrations of **10**, **11**, **18** or isofagomine. Each value represents the mean ± SEM (n = 3).

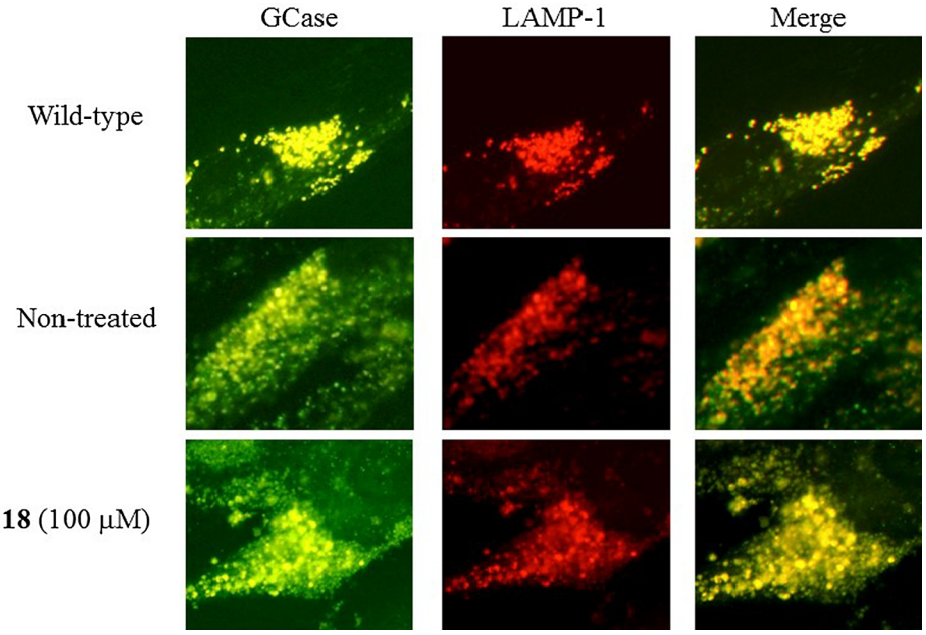

Fig. 8. Immunocytochemistry of GCase in wild type and N370S Gaucher fibroblasts double labeled with GCase antibody (green) and a lysosome marker (LAMP-1, red). Bright yellow (overlap of red and green) indicates increased levels of GCase in the lysosome. (For interpretation of the references to colour in this figure legend, the reader is referred to the web version of this article.)

H-1′b), 4.05 (td, 1H, $J_{4,3} = J_{4,5a} = 4.9$, $J_{4,5b} = 2.9$, H-4), 3.78 (dd, 1H, $J_{3,2} = 7.8$, H-3), 3.50 (td, 1H, H-2), 3.14 (dd, 1H, $^{2}J_{5a,5b} = 12.1$, H-5a), 2.87 (dd, 1H, H-5b). ^{13}C NMR (75.4 MHz, CD_3OD, δ ppm) δ 146.1 (C-4″), 136.7, 135.2 (C-1‴, C-3‴, C-5‴), 128.7 (C-4‴), 125.0 (C-2‴, C-6‴), 124.1 (C-5″), 76.3 (C-3), 72.3 (C-4), 62.7 (C-2), 54.3 (C-1′), 52.4 (C-5). HRESIMS *m/z* found 329.0566, calc. for $C_{13}H_{15}Cl_2N_4O_2$ $[M + H]^+$: 329.0567.

(2*S*,3*S*,4*R*)-2-[(4-(3,5-Dibromophenyl)-1*H*-1,2,3-triazol-1-yl) methyl]-pyrrolidine-3,4-diol (10): CuAAC (*Procedure 1*) using **26** [28] (25 mg, 0.16 mmol) and 1,3-dibromo-5-ethynylbenzene [47] followed by chromatography purification (CH_2Cl_2:MeOH:NH_4OH 6:1:0.1) yielded **10** (59 mg, 0.14 mmol, 88%) as a white solid. $[\alpha]_D^{25}$ – 18.0 (*c* 0.60, MeOH). IR (ν cm^{-1}) 3276, 3126 (OH, NH), 2923, 1599, 1557, 1405, 1095, 852, 742, 673. ^{1}H NMR (300 MHz, CD_3OD, δ ppm, *J* Hz) δ 8.45 (s, 1H, H-5″), 7.99 (d, 2H, $^{4}J_{H,H} = 1.7$, H-2‴, H-6‴), 7.68 (t, 1H, H-4‴), 4.67 (dd, 1H, $^{2}J_{1′a,1′b} = 14.0$, $J_{1′a,2} = 4.2$, H-1′a), 4.46 (dd, 1H, $J_{1′b,2} = 8.1$, H-1′b), 4.04 (td, 1H, $J_{4,3} = J_{4,5a} = 4.9$, $J_{4,5b} = 2.9$, H-4), 3.77 (dd, 1H, $J_{3,2} = 7.8$, H-3), 3.50 (td, 1H, H-2), 3.14 (dd, 1H, $^{2}J_{5a,5b} = 12.1$, H-5a), 2.86 (dd, 1H, H-5b). ^{13}C NMR (75.4 MHz, CD_3OD, δ ppm) δ 145.8 (C-4″), 135.7, 124.5 (C-1‴, C-3‴, C-5‴), 134.3 (C-4‴), 128.3 (C-2‴, C-6‴), 124.1 (C-5″), 76.3 (C-3), 72.3 (C-4), 62.7 (C-2), 54.3 (C-1′), 52.4 (C-5). HRESIMS *m/z* found 416.9554, calc. for $C_{13}H_{15}Br_2N_4O_2$ $[M + H]^+$: 416.9556.

(2*S*,3*S*,4*R*)-2-[(4-(3,5-Bis(trifluoromethyl)phenyl)-1*H*-1,2,3-triazol-1-yl)methyl]-pyrrolidine-3,4-diol (11): CuAAC (*Procedure 1*) using **26** [28] (25 mg, 0.16 mmol) and 1-ethynyl-3,5-bis(trifluoromethyl)benzene, followed by chromatography purification (CH_2Cl_2:MeOH:NH_4OH 6:1:0.1) yielded **11** (56 mg, 0.14 mmol, 88%) as a white solid. $[\alpha]_D^{24}$ – 24.2 (*c* 0.61, MeOH). IR (ν cm^{-1}) 3405, 3128 (OH, NH), 2954, 1427, 1277, 1134, 899, 702, 681. ^{1}H NMR (300 MHz, CD_3OD, δ ppm, *J* Hz) δ 8.63 (s, 1H, H-5″), 8.43 (br. s, 2H, H-2‴, H-6‴), 7.92 (br. s, 1H, H-4‴), 4.71 (dd, 1H, $^{2}J_{1′a,1′b} = 14.0$, $J_{1′a,2} = 4.3$, H-1′a), 4.49 (dd, 1H, $J_{1′b,2} = 8.1$, H-1′b), 4.05 (td, 1H, $J_{4,3} = J_{4,5a} = 4.9$, $J_{4,5b} = 2.9$, H-4), 3.79 (dd, 1H, $J_{3,2} = 7.8$, H-3), 3.52 (td, 1H, H-2), 3.15 (dd, 1H, $^{2}J_{5a,5b} = 12.1$, H-5a), 2.87 (dd, 1H, H-5b). ^{13}C NMR (75.4 MHz, CD_3OD, δ ppm, *J* Hz) δ 145.8 (C-4″), 134.7 (C-1‴), 133.5 (q, $^{2}J_{C,F} = 33.4$, C-3‴, C-5‴), 126.7–126.7 (m, C-2‴, C-6‴), 124.8 (q, $^{1}J_{C,F} = 271.5$, CF_3), 124.6 (C-5″), 122.4–122.1 (m, C-4‴), 76.3 (C-3), 72.4 (C-4), 62.7 (C-2), 54.4 (C-1′), 52.4 (C-5). HRESIMS *m/z* found 397.1086, calc. for $C_{15}H_{15}F_6N_4O_2$ $[M + H]^+$: 397.1094.

(2*S*,3*S*,4*R*)-2-[(4-(3,5-Dimethoxyphenyl)-1*H*-1,2,3-triazol-1-yl) methyl]-pyrrolidine-3,4-diol (12): CuAAC (*Procedure 1*) using **26** [28] (26 mg, 0.16 mmol) and 1-ethynyl-3,5-dimethoxybenzene, followed by chromatography purification (CH_2Cl_2:MeOH:NH_4OH 7:1:0.1→6:1:0.1) yielded **12** (45 mg, 0.14 mmol, 88%) as a white solid. $[\alpha]_D^{29}$ – 31.0 (*c* 0.57, MeOH). IR (ν cm^{-1}) 3434, 3262, (OH, NH), 2922, 1604, 1452, 1208, 1151, 1038, 834. ^{1}H NMR (300 MHz, CD_3OD, δ ppm, *J* Hz) δ 8.33 (s, 1H, H-5″), 6.99 (d, 2H, $^{4}J_{H,H} = 2.3$, H-2‴, H-6‴), 6.46 (t, 1H, H-4‴), 4.66 (dd, 1H, $^{2}J_{1′a,1′b} = 14.0$, $J_{1′a,2} = 4.2$, H-1′a), 4.44 (dd, 1H, $J_{1′b,2} = 8.1$, H-1′b), 4.04 (td, 1H, $J_{4,3} = J_{4,5a} = 4.9$, $J_{4,5b} = 2.9$, H-4), 3.82 (s, 6H, –OCH_3), 3.77 (dd, 1H, $J_{3,2} = 7.8$, H-3), 3.50 (td, 1H, H-2), 3.14 (dd, 1H, $^{2}J_{5a,5b} = 12.1$, H-5a), 2.86 (dd, 1H, H-5b). ^{13}C NMR (75.4 MHz, CD_3OD, δ ppm) δ 162.8 (C-3‴, C-5‴), 148.7 (C-4″), 133.4 (C-1‴), 123.3 (C-5″), 104.7 (C-2‴, C-6‴), 101.4 (C-4‴), 76.2 (C-3), 72.3 (C-4), 62.7 (C-2), 55.9 (–OCH_3), 54.2 (C-1′), 52.4 (C-5). HRESIMS *m/z* found 321.1555, calc. for $C_{15}H_{21}N_4O_4$ $[M + H]^+$: 321.1557.

(2*R*,3*S*,4*R*)-2-[(4-(4-Hydroxyphenyl)-1*H*-1,2,3-triazol-1-yl)methyl]-pyrrolidine-3,4-diol hydrochloride (13): CuAAC (*Procedure 2*) using **29** (81 mg, 0.27 mmol) and 4-ethynylphenol [44] followed by chromatography purification (EtOAc:cyclohexane 1:2→2:1) yielded (2*R*,3*S*,4*R*)-*N*-*tert*-butoxycarbonyl-2-[(4-(4-hydroxyphenyl)-1*H*-1,2,3-triazol-1-yl)methyl]-3,4-*O*-isopropylidene-pyrrolidine-3,4-diol (81 mg, 0.20 mmol, 74%) as a pale yellow solid. Subsequent acidic deprotection (44 mg, 0.11 mmol), yielded **13** (39 mg, 0.11 mmol, quant.) as a purple solid. $[\alpha]_D^{25}$ + 27.9 (*c* 0.69, MeOH). IR (ν cm^{-1}) 3132 (OH, NH), 2926, 1614, 1513, 1426, 1276, 1123, 834, 608. ^{1}H NMR (300 MHz, CD_3OD, δ ppm, *J* Hz) δ 8.68 (s, 1H, H-5″), 7.69 (d, 2H, $J_{H,H} = 8.6$, H-aromat.), 6.93 (d, 2H, H-aromat.), 5.17 (dd, 1H, $^{2}J_{1′a,1′b} = 15.0$, $J_{1′a,2} = 3.8$, H-1′a), 5.05–4.98 (m, 1H, H-1′b), 4.47 (td, 1H, $J_{4,5a} = J_{4,5b} = 7.0$, $J_{4,3} = 3.7$, H-4), 4.39 (t, 1H, $J_{3,2} = 3.8$, H-3), 4.34–4.29 (m, 1H, H-2), 3.50 (dd, 1H, $^{2}J_{5a,5b} = 11.6$, H-5a), 3.31–3.25 (m, 1H, H-5b). ^{13}C NMR (75.4 MHz, CD_3OD, δ ppm, *J* Hz) δ 160.7 (Cq aromat.), 147.3 (C-4″), 129.1 (C aromat.), 124.6 (C-5″), 118.7 (Cq aromat.), 117.2 (C aromat.), 72.1 (C-3), 71.6 (C-4), 61.6 (C-2), 50.6 (C-1′), 49.4 (C-5). HRESIMS *m/z* found 277.1296, calc. for $C_{13}H_{17}N_4O_3$ $[M]^+$: 277.1295.

(2*R*,3*S*,4*R*)-2-[(4-(4-Fluorophenyl)-1*H*-1,2,3-triazol-1-yl)methyl]-pyrrolidine-3,4-diol (16): CuAAC (*Procedure 2*) using **29** (74 mg, 0.25 mmol) and 1-ethynyl-4-fluorobenzene, followed by chromatography purification (EtOAc:cyclohexane 1:2) yielded (2*R*,3*S*,4*R*)-

N-*tert*-butoxycarbonyl-2-[(4-(4-fluorophenyl)-1*H*-1,2,3-triazol-1-yl)methyl]-3,4-*O*-isopropylidene-pyrrolidine-3,4-diol (86 mg, 0.21 mmol, 84%) as a white solid. Subsequent acidic deprotection (59 mg, 0.14 mmol) and purification on Dowex 50WX8 eluting with MeOH, H_2O and NH_4OH 25%, yielded **16** (20 mg, 0.072 mmol, 51%) as a white solid. $[\alpha]_D^{24}$ + 15.1 (*c* 0.60, MeOH). IR (ν cm^{-1}) 3398, 3253 (OH, NH), 2937, 1609, 1557, 1496, 1228, 1092, 841, 698. ^{1}H NMR (300 MHz, CD_3OD, δ ppm, *J* Hz) *δ* 8.31 (s, 1H, H-5″), 7.85–7.81 (m, 2H, H-aromat.), 7.20–7.14 (m, 2H, H-aromat.), 4.74 (dd, 1H, $^2J_{1'a,1'b}$ = 13.9, $J_{1'a,2}$ = 5.6, H-1′a), 4.50 (dd, 1H, $J_{1'b,2}$ = 8.3, H-1′b), 4.21 (td, 1H, $J_{4,5a}$ = $J_{4,5b}$ = 6.5, $J_{4,3}$ = 4.7, H-4), 4.07 (t, 1H, $J_{3,2}$ = 4.7, H-3), 3.68–3.61 (m, 1H, H-2), 3.07 (dd, 1H, $^2J_{5a,5b}$ = 11.1, H-5a), 2.89 (dd, 1H, H-5b). ^{13}C NMR (75.4 MHz, CD_3OD, δ ppm, *J* Hz) *δ* 164.1 (d, $^1J_{C,F}$ = 245.7, C-4‴), 147.7 (C-4″), 128.6 (d,$^3J_{C,F}$ = 8.2, C-2‴, C-6‴), 128.3 (d, $^4J_{C,F}$ = 3.3, C-1‴), 123.0 (C-5″), 116.8 (d, $^2J_{C,F}$ = 22.0, C-3‴, C-5‴), 73.7 (C-4), 73.1 (C-3), 61.6 (C-2), 52.2 (C-1′), 51.3 (C-5). HRESIMS *m/z* found 279.1253, calc. for $C_{13}H_{16}FN_4O_2$ $[M + H]^+$: 279.1252.

(2*R*,3*S*,4*R*)-2-[(4-(3,5-Difluorophenyl)-1*H*-1,2,3-triazol-1-yl)methyl]-pyrrolidine-3,4-diol (17): CuAAC (*Procedure 1*) using **30** [28] (32 mg, 0.20 mmol) and 1-ethynyl-3,5-difluorobenzene, followed by chromatography purification (CH_2Cl_2:MeOH:NH_4OH 6:1:0.1→5:1:0.1) yielded **17** (50 mg, 0.17 mmol, 85%) as a white solid. $[\alpha]_D^{25}$ + 25.2 (*c* 0.61, MeOH). IR (ν cm^{-1}) 3423, 3141 (OH, NH), 2926, 1627, 1595, 1435, 1223, 1123, 984, 838, 664. ^{1}H NMR (300 MHz, CD_3OD, δ ppm, *J* Hz) *δ* 8.42 (s, 1H, H-5″), 7.48–7.39 (m, 2H, H-2‴, H-6‴), 6.91 (tt, 1H, $J_{H,F}$ = 9.1, $^1J_{H,H}$ = 2.3, H-4‴), 4.75 (dd, 1H, $^2J_{1'a,1'b}$ = 13.9, $J_{1'a,2}$ = 5.5, H-1′a), 4.51 (dd, 1H, $J_{1'b,2}$ = 8.4, H-1′b), 4.21 (td, 1H, $J_{4,5a}$ = $J_{4,5b}$ = 6.6, $J_{4,3}$ = 4.6, H-4), 4.09 (t, 1H, $J_{3,2}$ = 4.7, H-3), 3.70–3.63 (m, 1H, H-2), 3.09 (dd, 1H, $^2J_{5a,5b}$ = 11.3, H-5a), 2.90 (dd, 1H, H-5b). ^{13}C NMR (75.4 MHz,CD_3OD, δ ppm, *J* Hz) *δ* 165.0 (dd, $^1J_{C,F}$ = 246.4, $^3J_{C,F}$ = 13.2, C-3‴, C-5‴), 146.5 (t, $^4J_{C,F}$ = 3.3, C-4″), 135.5 (t, $^3J_{C,F}$ = 10.6, C-1‴), 124.2 (C-5″), 109.5–109.2 (m, C-2‴, C-6‴), 104.0 (t, $^2J_{C,F}$ = 25.9, C-4‴), 73.6 (C-4), 73.0 (C-3), 61.5 (C-2), 52.1 (C-1′), 51.3 (C-5). HRESIMS *m/z* found 297.1157, calc. for $C_{13}H_{15}F_2N_4O_2$ $[M + H]^+$: 297.1158.

(2*R*,3*S*,4*R*)-2-[(4-(3,5-Dichlorophenyl)-1*H*-1,2,3-triazol-1-yl)methyl]-pyrrolidine-3,4-diol (18): CuAAC (*Procedure 1*) using **30** [28] (26 mg, 0.16 mmol) and 1,3-dichloro-5-ethynylbenzene [46] followed by chromatography purification (CH_2Cl_2:MeOH:NH_4OH 6:1:0.1→ 5:1:0.1) yielded **18** (47 mg, 0.14 mmol, 88%) as a white solid. $[\alpha]_D^{25}$ + 25.9 (*c* 0.55, MeOH). IR (ν cm^{-1}) 3272, 3127 (OH, NH), 2923, 1603, 1567, 1409, 1120, 852, 798, 673. ^{1}H NMR (300 MHz, CD_3OD, δ ppm, *J* Hz) *δ* 8.43 (s, 1H, H-5″), 7.80–7.79 (m, H-2‴, H-6‴), 7.40–7.38 (m, 1H, H-4‴), 4.75 (dd, 1H, $^2J_{1'a,1'b}$ = 13.9, $J_{1'a,2}$ = 5.5, H-1′a), 4.51 (dd, 1H, $J_{1'b,2}$ = 8.3, H-1′b), 4.21 (td, 1H, $J_{4,5a}$ = $J_{4,5b}$ = 6.6, $J_{4,3}$ = 4.6, H-4), 4.08 (t, 1H, $J_{3,2}$ = 4.7, H-3), 3.69–3.63 (m, 1H, H-2), 3.09 (dd, 1H, $^2J_{5a,5b}$ = 11.3, H-5a), 2.90 (dd, 1H, H-5b). ^{13}C NMR (75.4 MHz, CD_3OD, δ ppm) *δ* 146.0 (C-4″), 136.8, 135.2 (C-1‴, C-3‴, C-5‴), 128.7 (C-4‴), 125.0 (C-2‴, C-6‴), 124.3 (C-5″), 73.6 (C-4), 73.1 (C-3), 61.5 (C-2), 52.2 (C-1′), 51.3 (C-5). HRESIMS *m/z* found 329.0566, calc. for $C_{13}H_{15}Cl_2N_4O_2$ $[M + H]^+$: 329.0567.

(2*R*,3*S*,4*R*)-2-[(4-(3,5-Dibromophenyl)-1*H*-1,2,3-triazol-1-yl)methyl]-pyrrolidine-3,4-diol (19): CuAAC (*Procedure 1*) using **30** [28] (25 mg, 0.16 mmol) and 1,3-dibromo-5-ethynylbenzene [47] followed by chromatography purification (CH_2Cl_2:MeOH:NH_4OH 6:1:0.1) yielded **19** (52 mg, 0.12 mmol, 75%) $[\alpha]_D^{25}$ + 14.7 (*c* 0.62, MeOH). IR (ν cm^{-1}) 3277 (OH, NH), 2927, 1602, 1557, 1409, 1229, 1103, 852, 742, 621. ^{1}H NMR (300 MHz, CD_3OD, δ ppm, *J* Hz) *δ* 8.42 (s, 1H, H-5″), 7.98 (d, 2H, $^4J_{H,H}$ = 1.7, H-2‴, H-6‴), 7.67 (t, 1H, H-4‴), 4.74 (dd, 1H, $^2J_{1'a,1'b}$ = 13.9, $J_{1'a,2}$ = 5.6, H-1′a), 4.51 (dd, 1H, $J_{1'b,2}$ = 8.3, H-1′b), 4.21 (td, 1H, $J_{4,5a}$ = $J_{4,5b}$ = 6.6, $J_{4,3}$ = 4.6, H-4), 4.08 (t, 1H, $J_{3,2}$ = 4.7, H-3), 3.68–3.62 (m, 1H, H-2), 3.08 (dd, 1H, $^2J_{5a,5b}$ = 11.2, H-5a), 2.90 (dd, 1H, H-5b). ^{13}C NMR (75.4 MHz, CD_3OD, δ ppm) *δ* 145.7 (C-4″), 135.7, 124.5 (C-1‴, C-3‴, C-5‴), 134.3 (C-4‴), 128.3 (C-2‴, C-6‴), 124.2 (C-5″), 73.5 (C-4), 73.1 (C-3), 61.5 (C-2), 52.2 (C-1′), 51.3 (C-5). HRESIMS *m/z* found 416.9554, calc. for $C_{13}H_{15}Br_2N_4O_2$ $[M + H]^+$: 416.9556.

(2*R*,3*S*,4*R*)-2-[(4-(3,5-Bis(trifluoromethyl)phenyl)-1*H*-1,2,3-triazol-1-yl)methyl]-pyrrolidine-3,4-diol (20): CuAAC (*Procedure 1*) using **30** [28] (26 mg, 0.16 mmol) and 1-ethynyl-3,5-bis(trifluoromethyl)benzene, followed by chromatography purification (CH_2Cl_2:MeOH:NH_4OH 7:1:0.1→6:1:0.1) yielded **20** (54 mg, 0.14 mmol, 88%) as a white solid. $[\alpha]_D^{24}$ + 19.3 (*c* 0.55, MeOH). IR (ν cm^{-1}) 3287, 3144 (OH, NH), 2935, 1657, 1465, 1277, 1127, 896, 700, 681. ^{1}H NMR (300 MHz, CD_3OD, δ ppm, *J* Hz) *δ* 8.61 (s, 1H, H-5″), 8.42 (br. s, 2H, H-2‴, H-6‴), 7.91 (br. s, 1H, H-4‴), 4.78 (dd, 1H, $^2J_{1'a,1'b}$ = 13.9, $J_{1'a,2}$ = 5.6, H-1′a), 4.54 (dd, 1H, $J_{1'b,2}$ = 8.4, H-1′b), 4.22 (td, 1H, $J_{4,5a}$ = $J_{4,5b}$ = 6.5, $J_{4,3}$ = 4.6, H-4), 4.10 (t, 1H, $J_{3,2}$ = 4.7, H-3), 3.71–3.63 (m, 1H, H-2), 3.09 (dd, 1H, $^2J_{5a,5b}$ = 11.3, H-5a), 2.91 (dd, 1H, H-5b). ^{13}C NMR (75.4 MHz, CD_3OD, δ ppm, *J* Hz) *δ* 145.7 (C-4″), 134.7 (C-1‴), 133.5 (q, $^2J_{C,F}$ = 33.4, C-3‴, C-5‴), 126.7–126.7 (m, C-2‴, C-6‴), 124.8 (q, $^1J_{C,F}$ = 271.6, CF_3), 124.7 (C-5″), 122.4–122.2 (m, C-4‴), 73.7 (C-4), 73.1 (C-3), 61.5 (C-2), 52.3 (C-1′), 51.4 (C-5). HRESIMS *m/z* found 397.1087, calc. for $C_{15}H_{15}F_6N_4O_2$ $[M + H]^+$: 397.1094.

(2*R*,3*S*,4*R*)-2-[(4-(3,5-Dimethoxyphenyl)-1*H*-1,2,3-triazol-1-yl)methyl]-pyrrolidine-3,4-diol (21): CuAAC (*Procedure 1*) using **30** [28] (26 mg, 0.16 mmol) and 1-ethynyl-3,5-dimethoxybenzene, followed by chromatography purification (CH_2Cl_2:MeOH:NH_4OH 7:1:0.1→6:1:0.1) yielded **21** (41 mg, 0.13 mmol, 81%) as a pale yellow solid. $[\alpha]_D^{29}$ + 26.3 (*c* 0.58, DMSO). IR (ν cm^{-1}) 3269, 3125, (OH, NH), 2916, 1595, 1474, 1203, 1154, 1065, 826, 684. ^{1}H NMR (300 MHz, DMSO-d_6, δ ppm, *J* Hz) *δ* 8.53 (s, 1H, H-5″), 7.02 (d, 2H, $^4J_{H,H}$ = 2.3, H-2‴, H-6‴), 6.45 (t, 1H, H-4‴), 4.81–4.75 (m, 2H, OH-3, OH-4), 4.52 (dd, 1H, $^2J_{1'a,1'b}$ = 13.6, $J_{1'a,2}$ = 4.8, H-1′a), 4.28 (dd, 1H, $J_{1'b,2}$ = 8.9, H-1′b), 4.03–3.91 (m, 2H, H-3, H-4), 3.79 (s, 6H, –OCH_3), 3.52–3.45 (m, 1H, H-2), 3.28 (br. s, 1H, NH), 2.95 (dd, 1H, $^2J_{5a,5b}$ = 10.8, $J_{5a,4}$ = 6.6, H-5a), 2.68 (dd, 1H, $J_{5b,4}$ = 6.4, H-5b). ^{13}C NMR (75.4 MHz, DMSO-d_6, δ ppm) *δ* 160.8 (C-3‴, C-5‴), 145.8 (C-4″), 132.9 (C-1‴), 122.4 (C-5″), 103.0 (C-2‴, C-6‴), 99.7 (C-4‴), 72.2 (C-4), 71.8 (C-3), 59.8 (C-2), 55.3 (–OCH_3), 51.3 (C-1′), 50.4 (C-5). HRESIMS *m/z* found 321.1554, calc. for $C_{15}H_{21}N_4O_4$ $[M + H]^+$: 321.1557.

(3*S*,4*S*,5*S*)-*N*-*tert*-Butoxycarbonyl-5-azidomethyl-3,4-*O*-isopropylidene-pyrrolidine-2-one-3,4-diol (31): A solution of **25** [28] (128 mg, 0.429 mmol) in EtOAc (3.5 mL) was added to a solution of $NaIO_4$ (277 mg, 1.28 mmol) and $RuO_2{\cdot}xH_2O$ (57 mg, 0.43 mmol) in water (3.5 mL). The mixture was vigorously stirred for 48 h and then, it was filtered through celite and evaporated. Chromatography purification on silica gel (EtOAc:cyclohexane 1:4) yielded **31** (108 mg, 0.346 mmol, 81%) as a colourless oil. $[\alpha]_D^{22}$ + 57.9 (*c* 0.52, CH_2Cl_2). IR (ν cm^{-1}) 2109 (N_3), 1716 (C═O), 1148, 1095, 977, 844, 640, 604. ^{1}H NMR (300 MHz, $CDCl_3$, δ ppm, *J* Hz) *δ* 4.74 (d, 1H $J_{3,4}$ = 5.5, H-3 or H-4), 4.43 (d, 1H, H-4 or H-3), 4.29–4.27 (m, 1H, H-5), 3.87 (dd, 1H, $^2J_{1'a,1'b}$ = 12.8, $J_{1'a,5}$ = 3.7, H-1′a), 3.63 (dd, 1H, $J_{1'b,5}$ = 2.2, H-1′b), 1.55 (s, 9H, -C(CH_3)$_3$), 1.44 (s, 3H, -C(CH_3)$_2$), 1.36 (s, 3H, -C(CH_3)$_2$). ^{13}C NMR (75.4 MHz, $CDCl_3$, δ ppm) *δ* 170.5 (C═O), 150.0 (C═O, Boc), 112.6 (-*C*(CH$_3$)$_2$), 84.5 (-*C*(CH$_3$)$_3$), 77.7, 75.4 (C-3, C-4), 59.6 (C-5), 51.9 (C-1′), 28.1 (-C(CH_3)$_3$), 27.2 (-C(CH_3)$_2$), 25.7 (-C(CH_3)$_2$). HRESIMS *m/z* found 335.1323, calc. for $C_{13}H_{20}O_5N_4$ $[M + H]^+$: 335.1326.

(3*S*,4*S*,5*S*)-5-[(4-Phenyl-1*H*-1,2,3-triazol-1-yl)methyl]-pyrrolidine-2-one-3,4-diol (22): CuAAC (*Procedure 2*) using **31** (53 mg, 0.17 mmol) and phenylacetylene, followed by chromatography purification (EtOAc:cyclohexane 1:2) yielded (3*S*,4*S*,5*S*)-*N*-*tert*-butoxycarbonyl-5-[(4-phenyl-1*H*-1,2,3-triazol-1-yl)methyl]-3,4-*O*-isopropylidene-pyrrolidine-2-one-3,4-diol (59 mg, 0.14 mmol, 82%) as a white solid. Subsequent acidic deprotection (79 mg, 0.19 mmol) and chromatographic purification on silica gel (CH_2Cl_2:MeOH 10:1→5:1), yielded **22** (37 mg, 0.14 mmol, 74%) as a white solid. $[\alpha]_D^{23}$ + 150.2 (*c* 0.66, MeOH). IR (ν cm^{-1}) 3359 (OH, NH), 1706 (C═O), 1452, 1140, 1050, 992, 772, 626. ^{1}H NMR (300 MHz, CD_3OD, δ ppm, *J* Hz) *δ* 8.32 (s, 1H, H-5″), 7.84–7.80 (m, 2H, H-aromat.), 7.47–7.41 (m, 2H, H-

aromat.), 7.38–7.32 (m, 1H, H-aromat.), 4.64 (d, 2H, $J_{1',5}$ = 5.6, H-1′), 4.28 (dd, 1H, $J_{4,3}$ = 5.3, $J_{4,5}$ = 1.1, H-4), 3.95 (td, 1H, H-5), 3.86 (d, 1H, H-3). ^{13}C NMR (75.4 MHz, CD_3OD, δ ppm) δ 178.0 (C═O), 149.1 (C-4″), 131.5 (Cq aromat.), 130.0 (C aromat.), 129.5 (C aromat.), 126.7 (C aromat.), 123.3 (C-5″), 71.5 (C-3), 70.6 (C-4), 61.0 (C-5), 52.9 (C-1′). HRESIMS *m/z* found 275.1142, calc. for $C_{13}H_{15}O_3N_4$ $[M + H]^+$: 275.1139.

(3*S*,4*S*,5*S*)-5-[(4-(3,5-Difluorophenyl)-1*H*-1,2,3-triazol-1-yl) methyl] -pyrrolidine-2-one-3,4-diol (23): CuAAC (*Procedure 2*) using **31** (61 mg, 0.20 mmol) and 1-ethynyl-3,5-difluorobenzene, followed by chromatography purification (EtOAc:cyclohexane 1:2) yielded (3*S*,4*S*,5*S*)-*N*-*tert*-butoxycarbonyl-5-[(4-(3,5-difluorophenyl)-1*H*-1,2,3-triazol-1-yl)methyl]-3,4-*O*-isopropylidene-pyrrolidine-2-one-3,4-diol (77 mg, 0.17 mmol, 85%) as a white solid. Subsequent acidic deprotection (66 mg, 0.15 mmol) and chromatographic purification on silica gel (CH_2Cl_2:MeOH 7:1→5:1), yielded **23** (34 mg, 0.11 mmol, 73%) as a white solid. $[\alpha]_D^{23}$ – 34.3 (*c* 0.56, MeOH). IR (ν cm^{-1}) 3249 (OH, NH), 1696 (C═O), 1595, 1120, 986, 848. ^{1}H NMR (300 MHz, CD_3OD, δ ppm, *J* Hz) δ 8.44 (s, 1H, H-5″), 7.49–7.40 (m, 2H, H-2‴, H-6‴), 6.93 (tt, 1H, $J_{H,F}$ = 9.1, $^4J_{H,H}$ = 2.3, H-4‴), 4.65 (d, 2H, $J_{1',5}$ = 5.8, H-1′), 4.28 (dd, 1H, $J_{4,3}$ = 5.3, $J_{4,5}$ = 1.0, H-4), 3.96 (td, 1H, H-5), 3.91 (d, 1H, H-3). ^{13}C NMR (75.4 MHz, CD_3OD, δ ppm) δ 178.0 (C═O), 165.0 (dd, $^1J_{C,F}$ = 246.6, $^3J_{C,F}$ = 13.2, C-3‴, C-5‴), 147.0 (t, $^4J_{C,F}$ = 3.2, C-4″), 135.2 (t, $^3J_{C,F}$ = 10.6, C-1‴), 124.3 (C-5″), 109.6–109.3 (m, C-2‴, C-6‴), 104.2 (t, $^2J_{C,F}$ = 25.9, C-4‴), 71.5 (C-3), 70.7 (C-4), 61.0 (C-5), 53.0 (C-1′). HRESIMS *m/z* found 333.0768, calc. for $C_{13}H_{12}O_3N_4F_2$ $[M + H]^+$: 333.0770.

(2*S*,3*S*,4*R*,5*R*)-2-Azidomethyl-5-hydroxymethyl-pyrrolidine-3,4-diol (33): To a solution of **32** [37] (62 mg, 0.38 mmol) in H_2O (1 mL), MeOH (1 mL), $NaHCO_3$ (128 mg, 1.52 mmol), $CF_3(CF_2)_3SO_2N_3$ [48] (185 mg, 0.569 mmol) in Et_2O (1 mL) and $CuSO_4{\cdot}5H_2O$ (10 mg, 0.040 mmol) were added. After stirring at r.t. for 3.5 h, the solvent was removed in vacuo and the resulting residue was dissolved in MeOH and stirred with Quadrasil® MP for 1.5 h. Then, the solids were filtered through celite and the solvent was evaporated. Treatment with HCl (1 M) and purification on Dowex 50WX8 eluting with MeOH, H_2O and NH_4OH 33%, yielded **33** (45 mg, 0.24 mmol, 63%) as a pale yellow oil. $[\alpha]_D^{29}$ – 12.0 (*c* 0.84, MeOH). IR (ν cm^{-1}) 3299 (OH, NH), 2924, 2098 (N_3), 1440, 1270, 1102, 944, 733. ^{1}H NMR (300 MHz, CD_3OD, δ ppm, *J* Hz) δ 3.82 (ap. t, 1H, H-4), 3.72–3.54 (m, 4H, H-3, –C*H*$_2$OH, H-1′a), 3.41 (dd, 1H, $^2J_{1'b,1'a}$ = 12.5, $J_{1'b,2}$ = 6.2, H-1′b), 3.14 (td, 1H, $J_{2,3}$ = 6.2, $J_{2,1'a}$ = 4.3, H-2), 3.07 (ap. q, 1H, H-5). ^{13}C NMR (75.4 MHz, CD_3OD, δ ppm) δ 74.5 (C-3), 73.5 (C-4), 66.2 (C-5), 63.5 (–*C*H$_2$OH), 63.4 (C-2), 54.5 (C-1′). HRESIMS *m/z* found 189.0979, calc. for $C_6H_{13}N_4O_3$ $[M + H]^+$: 189.0982.

(2*S*,3*S*,4*R*,5*R*)-2-[(4-Phenyl-1*H*-1,2,3,-triazol-1-yl)methyl] -5-hydroxymethyl-pyrrolidine-3,4-diol (24): CuAAC (*Procedure 1*) using **33** (30 mg, 0.16 mmol) and phenylacetylene, followed by chromatography purification (CH_2Cl_2:MeOH:NH_4OH 5:1:0.1→4:1:0.1) yielded **24** (30 mg, 0.10 mmol, 63%) as a white solid. $[\alpha]_D^{29}$ – 24.1 (*c* 0.67, MeOH). IR (ν cm^{-1}) 3249, 3122, (OH, NH), 2918, 1653, 1426, 1225, 1107, 1051, 909, 765. ^{1}H NMR (300 MHz, CD_3OD, δ ppm, *J* Hz) δ 8.38 (s, 1H, H-5″), 7.83–7.79 (m, 2H, H-aromat.), 7.46–7.38 (m, 2H, H-aromat.), 7.34 (ap. tt, 1H, H-aromat.), 4.64 (dd, 1H, $^2J_{1'a,1'b}$ = 13.9, $J_{1'a,2}$ = 4.2, H-1′a), 4.49 (dd, 1H, $J_{1'b,2}$ = 7.3, H-1′b), 3.78–3.72 (m, 2H, H-4, H-3), 3.58–3.46 (m, 3H, H-2, –C*H*$_2$OH), 3.15–3.11 (m, 1H, H-5). ^{13}C NMR (75.4 MHz, CD_3OD, δ ppm) δ 148.7 (C-4″), 131.8 (Cq aromat.), 130.0 (C aromat.), 129.3 (C aromat.), 126.7 (C aromat.), 123.3 (C-5″), 74.8, 73.5 (C-3, C-4), 66.0 (C-5), 64.1 (–*C*H$_2$OH), 63.4 (C-2), 54.3 (C-1′). HRESIMS *m/z* found 291.1454, calc. for $C_{14}H_{19}N_4O_3$ $[M + H]^+$: 291.1452.

4.2. Inhibition studies with commercial enzymes

The % of inhibition towards the corresponding glycosidase was determined in the presence of 1.0 mM of the inhibitor on the well. Each enzymatic assay (final volume 0.12 mL) contains 0.01–0.5 units/mL of the enzyme and 4.2 mM aqueous solution of the appropriate *p*-nitrophenyl glycopyranoside (substrate) buffered to the optimal pH of the enzyme. Enzyme and inhibitor were pre-incubated for 5 min at r.t., and the reaction started by addition of the substrate. After 20 min of incubation at 37 °C, the reaction was stopped by addition of 0.1 mL of sodium borate solution (pH 9.8). The *p*-nitrophenolate formed was measured by visible absorption spectroscopy at 405 nm. Under these conditions, the *p*-nitrophenolate released led to optical densities linear with both reaction time and concentration of the enzyme. The IC_{50} value (concentration of inhibitor required for 50% inhibition of enzyme activity) was determined from plots of % inhibition *versus* different inhibitor concentrations. The IC_{50} is determined by duplicate (< 10% of difference) and the average value is given.

4.3. Inhibition studies with lysosomal enzymes

The inhibitory activity toward human lysosomal β-glucocerebrosidase and α-galactosidase A was measured with 4-methylumbelliferyl-β-D-glucopyranoside and 4-methylumbelliferyl-α-D-galactopyranoside as substrate. The reaction mixture consisted on 100 mM McIlvaine buffer (pH 5.2), 0.25% sodium taurocholate and 0.1% Triton X-100, and the appropriate amount of enzyme. The reaction mixture was pre-incubated at 0 °C for 45 min, and the reaction was started by adding 3 mM substrate solution, followed by incubation at 37 °C for 30 min. The reaction was stopped by the addition of 1.6 mL of the solution of 400 mM glycine-NaOH solution (pH 10.6). The released 4-methylumbelliferone was measured (excitation 362 nm, emission 450 nm) with a F-4500 fluorescence spectrophotometer (Hitachi, Tokyo, Japan). The IC_{50} is determined by duplicate (less than 10% of difference) and the average value is given.

4.4. X-ray crystallography and docking studies

Lyophilized GCase (Cerezyme ®, Genzyme Corporation) was partially deglycosylated with PNGase F (Promega) as previously described [49]. Crystals were grown at room temperature in hanging drop format from 6 mg/mL GCase in phosphate-buffered saline in a 1:1 ratio with mother liquor (0.1 M HEPES pH 7.5, 0.8 M NaH_2PO_4 and 0.8 M KH_2PO_4) [49]. Prior to data collection, crystal drops were incubated for 1 h with 1.25 mM compound **18** at room temperature, cryo-protected by transfer into mother liquor including 20% glycerol, then cooled in liquid nitrogen.

Crystallographic data were collected at SER-CAT ID-22 beamline at the Advanced Photon Source using an EIGER 16 M detector, then processed using XDS [50]. Molecular replacement was conducted in Phenix using a monomeric search model derived from the amino acid chain of PDB 2NSX bound to IFG. Models were iteratively built and refined using Phenix and Coot [51].

Docking calculations were carried out using DockingServer [41]. The MMFF94 force field [52] was used for energy minimization of pyrrolidine-triazole **11** using DockingServer. Gasteiger partial charges were added to the ligand atoms. Non-polar hydrogen atoms were merged, and rotatable bonds were defined. Docking calculations were carried out upon a protein model derived from PDB 6MOZ Chain A. Essential hydrogen atoms, Kollman united atom type charges, and solvation parameters were added with the aid of AutoDock tools [53]. Affinity (grid) maps of 40 × 40 × 40 Å grid points and 0.375 Å spacing were generated using the Autogrid program [52]. AutoDock parameter set- and distance-dependent dielectric functions were used to calculate van der Waals and the electrostatic terms, respectively. All electrostatics were calculated at pH 7.

Docking simulations were performed using the Lamarckian genetic algorithm (LGA) and the Solis & Wets local search method [54]. Initial position, orientation, and torsions of the ligand molecules were set at random. Each docking experiment was derived from 100 different runs

set to terminate after a maximum of 2.5 million energy evaluations. The population size was set to 150. During the search, a translational step of 0.2 Å, and quaternion and torsion steps of 5 were applied.

Figures were generated using PyMol (Schrodinger). Ligand interactions were further investigated using LigPlot + v. 1.4 [55]. Core alignments of previous structures were conducted using the SSM superimpose function in Coot. The structure has been deposited in the PDB under accession code 6MOZ.

4.5. Pharmacological chaperone activity

The Gaucher's cell line with β-glucocerebrosidase mutation of N370S was obtained from the Coriell Cell Repositories (Camden, NJ). The Gaucher N370S fibroblasts were cultured in EMEM (Eagle's Minimum Essential Medium; Sigma-Aldrich Co) supplemented with 15% FCS. Cells were cultured in a water-jacket incubator at 37°C under 5% CO_2 in the presence or absence of samples for 6 days. After washing twice with a medium, the cell pellet were homogenized in a citrate buffer (pH 5.2) containing 0.25% sodium taurochole and 0.1% Triton X-100. The supernatant obtained from the homogenate after centrifugation at 1000 g for 5 min was subject to enzyme assays and protein determination. Intercellular β-glucocerebrosidase activities were determined with 4-methylumbelliferyl-β-D-glucoside as substrate at pH 5.2.

4.6. Immunocytochemistry

The Gaucher's cell line with GCase mutation of N370S was treated with rabbit polyclonal anti-GCase serum as a primary antibody for the detection of GCase, and monoclonal anti-LAMP-1 serum for the detection of lysosomes. Hilyte Fluor™ 488-conjugated goat anti-rabbit IgG serum and Alexa Fluor™ 594-conjugated goat anti-rat IgG serum were used as secondary antibodies. Gaucher fibroblasts were grown on sterile coverslips with presence or absence of the iminosugar and cultured with 5 days in EMEM. All immunocytochemistry procedures were performed at room temperature. After cells had been washed three times with PBS, they were fixed with 1 mL of 4% paraformaldehyde in PBS for 20 min, and then washed three times with PBS. The cells were permeated with 1 mL of 0.01% Triton X-100 in PBS for 20 min, and then washed three times with PBS. After a 20 min treatment with 1 mL of blocking solution (5% skim milk in PBS), the cells were incubated with the primary antibody diluted in 1% skim milk in PBS for 30 min, and this was followed by three washes with 1 mL of PBS. Coverslips were then incubated in the dark with the secondary antibody diluted in 1% skim milk in PBS for 30 min, and this was followed by three washes with 1 mL of PBS. The coverslips were mounted with a drop of SlowFade™ Diamond, and fluorescence was visualized using an Olympus fluorescence microscope.

5. Notes

The authors declare no competing financial interest.

Acknowledgments

This work was supported by the Ministerio de Economía y Competitividad of Spain (CTQ2016-77270-R), the Consejería de Economía y Conocimiento-Junta de Andalucía (FQM-345), a Grant-in-Aid for Scientific Research (C) from the Japanese Society for the Promotion of Science (JSPS KAKENHI Grant Number JP17K08362) (AK) and by the U. S. National Institutes of Health F32AG027647 and R01EY021205 (RLL). M. Martínez-Bailén acknowledges the Spanish government for a FPU fellowship and the group of Dr. F. Cardona (synthesis of 32). We thank CITIUS-University of Seville (MS and NMR services), C. Vago, and Y. Ajirniar (crystallization) for technical assistance.

Appendix A. Supplementary material

Supplementary data to this article can be found online at https://doi.org/10.1016/j.bioorg.2019.02.025.

References

[1] F.M. Platt, Sphingolipid lysosomal storage disorders, Nature 510 (2014) 68–75.
[2] L. Smith, S. Mullin, A.H.V. Schapira, Insights into the structural biology of Gaucher disease, Exp. Neurol. 298 (2017) 180–190.
[3] E. Sidransky, M.A. Nalls, J.O. Aasly, J. Aharon-Peretz, G. Annesi, E.R. Barbosa, A. Bar-Shira, D. Berg, J. Bras, A. Brice, et al., Multicenter analysis of glucocerebrosidase mutations in Parkinson's disease, N. Engl. J. Med. 361 (2009) 1651–1661.
[4] D.M. Pereira, P. Valentao, P.B. Andrade, Tuning protein folding in lysosomal storage diseases: the chemistry behind pharmacological chaperones, Chem. Sci. 9 (2018) 1740–1752.
[5] J.-Q. Fan, A contradictory treatment for lysosomal storage disorders: inhibitors enhance mutant enzyme activity, Trends Pharmacol. Sci. 24 (2003) 355–360.
[6] M. Convertino, J. Das, N.V. Dokholyan, Pharmacological chaperones: design and development of new therapeutic strategies for the treatment of conformational diseases, ACS Chem. Biol. 11 (2016) 1471–1489.
[7] J.-Q. Fan, A counterintuitive approach to treat enzyme deficiencies: use of enzyme inhibitors for restoring mutant enzyme activity, Biol. Chem. 389 (2008) 1–11.
[8] E.M. Sánchez-Fernández, J.M. García-Fernández, C. Ortiz-Mellet, Glycomimetic-based pharmacological chaperones for lysosomal storage disorders: lessons from Gaucher, GM1-gangliosidosis and Fabry diseases, Chem. Commun. 52 (2016) 5497–5515.
[9] A. Markham, Migalastat: first global approval, Drugs 76 (2016) 1147–1152.
[10] C.D. Navo, F. Corzana, E.M. Sánchez-Fernández, J.H. Busto, A.M. Avenoza, M.M. Zurbano, E. Nanba, K. Higaki, C. Ortiz Mellet, J.M. García Fernández, J.M. Peregrina, Conformationally-locked *C*-glycosides: tuning aglycone interactions for optimal chaperone behaviour in Gaucher fibroblasts, Org. Biomol. Chem. 14 (2016) 1473–1484.
[11] E.D. Goddard-Borger, M.B. Tropak, S. Yonekawa, C. Tysoe, D.J. Mahuran, S.J. Withers, Rapid assembly of a library of lipophilic imino-sugars via the thiol-ene reaction yields promising pharmacological chaperones for the treatment of Gaucher disease, J. Med. Chem. 55 (2012) 2737–2745.
[12] C. Parmeggiani, S. Catarzi, C. Matassini, G. D'Adamio, A. Morrone, A. Goti, P. Paoli, F. Cardona, Human acid β-glucosidase inhibition by carbohydrate derived imino-sugars: towards new pharmacological chaperones for Gaucher disease, ChemBioChem 16 (2015) 2054–2064.
[13] W.-C. Cheng, C.-Y. Wenga, W.-Y. Yun, S.-Y. Chang, Y.-C. Lin, F.-J. Tsai, F.-Y. Huang, Y.-R. Chen, Rapid modifications of *N*-substitution in imino-sugars: Development of new β-glucocerebrosidase inhibitors and pharmacological chaperones for Gaucher disease, Bioorg. Med. Chem. 21 (2013) 5021–5028.
[14] J. Serra-Vinardell, L. Díaz, H. Gutiérrez-de-Teránd, G. Sánchez-Ollé, J. Bujons, H. Michelakakis, I. Mavridou, J.M.F.G. Aerts, A. Delgado, D. Grinberg, L. Vilageliu, J. Casas, Selective chaperone effect of aminocyclitol derivatives on G202R and other mutant glucocerebrosidases causing Gaucher disease, Int. J. Biochem. Cell Biol. 54 (2014) 245–254.
[15] S. Patnaik, W. Zheng, J.-H. Choi, O. Motabar, N. Southall, W. Westbroek, W.A. Lea, A. Velayati, E. Goldin, E. Sidransky, W. Leister, J.J. Marugan, Discovery, structure-activity relationship, and biological evaluation of noninhibitory small molecule chaperones of glucocerebrosidase, J. Med. Chem. 55 (2012) 5734–5748.
[16] E. Laigre, D. Hazelard, J. Casas, J. Serra-Vinardell, H. Michelakakis, I. Mavridou, J.M.F.G. Aerts, A. Delgado, P. Compain, Investigation of original multivalent iminosugars as pharmacological chaperones for the treatment of Gaucher disease, Carbohydr. Res. 429 (2016) 98–104.
[17] T. Mena-Barragán, A. Narita, D. Matias, G. Tiscornia, E. Nanba, K. Ohno, Y. Suzuki, K. Higaki, J.M. Garcia-Fernandez, C. Ortiz Mellet, pH-Responsive pharmacological chaperones for rescuing mutant glycosidases, Angew. Chem. Int. Ed. 54 (2015) 11696–11700.
[18] A. Trapero, A. Llebaria, Glucocerebrosidase inhibitors: future drugs for the treatment of Gaucher disease? Future Med. Chem. 6 (2014) 975–978.
[19] R. Khanna, E.R. Benjamin, L. Pellegrino, A. Schilling, B.A. Rigat, R. Soska, H. Nafar, B.E. Ranes, J. Feng, Y. Lun, A.C. Powe, D.J. Palling, B.A. Wustman, R. Schiffmann, D.J. Mahuran, D.J. Lockhart, K.J. Valenzano, The pharmacological chaperone isofagomine increases the activity of the Gaucher disease L444P mutant form of β-glucosidase, FEBS J. 277 (2010) 1618–1638.
[20] P. Alfonso, S. Pampin, J. Estrada, J.C. Rodriguez-Rey, P. Giraldo, J. Sancho, M. Pocovi, Miglustat (NB-DNJ) works as a chaperone for mutated acid β-glucosidase in cells transfected with several Gaucher disease mutations, Blood Cells Mol. Dis. 35 (2005) 268–276.
[21] A.R. Sawkar, W.C. Cheng, E. Beutler, C.H. Wong, W.E. Balch, J.W. Kelly, Chemical chaperones increase the cellular activity of N370S β-glucosidase: a therapeutic strategy for Gaucher disease, Proc. Natl. Acad. Sci. U. S. A. 99 (2002) 15428–15433.
[22] A. Zimran, G. Altarescu, D. Elstein, Pilot study using ambroxol as a pharmacological chaperone in type 1 Gaucher disease, Blood Cells Mol. Dis. 50 (2013) 134–137.
[23] A. Narita, K. Shirai, S. Itamura, A. Matsuda, A. Ishihara, K. Matsushita, C. Fukuda, N. Kubota, R. Takayama, H. Shigematsu, et al., Ambroxol chaperone therapy for neuronopathic Gaucher disease: a pilot study, Ann. Clin. Transl. Neurol. 3 (2016) 200–215.
[24] O. Jung, S. Patnaik, J. Marugan, E. Sidransky, W. Westbroek, Progress and potential

of non-inhibitory small molecule chaperones for the treatment of Gaucher disease and its implications for Parkinson disease, Expert Rev. Proteom. 13 (2016) 471–479.
[25] P. Compain, O.R. Martin, C. Boucheron, G. Godin, L. Yu, K. Ikeda, N. Asano, Design and synthesis of highly potent and selective pharmacological chaperones for the treatment of Gaucher's disease, ChemBioChem 7 (2006) 1356–1359.
[26] A. Kato, I. Nakagome, K. Sato, A. Yamamoto, I. Adachi, R.J. Nash, G.W.J. Fleet, Y. Natori, Y. Watanabe, T. Imahori, Y. Yoshimura, H. Takahatae, S. Hirono, Docking study and biological evaluation of pyrrolidine-based iminosugars as pharmacological chaperones for Gaucher disease, Org. Biomol. Chem. 14 (2016) 1039–1048.
[27] T. Mena-Barragan, M.I. Garcia-Moreno, E. Nanba, K. Higaki, A.L. Concia, P. Clapes, J.M. Garcia Fernandez, C. Ortiz-Mellet, Inhibitor versus chaperone behaviour of D-fagomine, DAB and LAB sp^2-iminosugar conjugates against glycosidases: a structure-activity relationship study in Gaucher fibroblasts, Eur. J. Med. Chem. 121 (2016) 880–891.
[28] M. Martínez-Bailén, A.T. Carmona, E. Moreno-Clavijo, I. Robina, D. Ide, A. Kato, A.J. Moreno-Vargas, Tuning of β-glucosidase and α-galactosidase inhibition by generation and *in situ* screening of a library of pyrrolidine-triazole hybrid molecules, Eur. J. Med. Chem. 138 (2017) 532–542.
[29] A.J. Moreno-Vargas, R. Demange, J. Fuentes, I. Robina, P. Vogel, Synthesis of [(2*S*,3*S*,4*R*)-3,4-dihydroxypyrrolidin-2-yl]-5-methylfuran-4-carboxylic acid derivatives: new leads as selective β-galactosidase inhibitors, Bioorg. Med. Chem. Lett. 12 (2002) 2335–2339.
[30] A.J. Moreno-Vargas, A.T. Carmona, F. Mora, P. Vogel, I. Robina, Stereoselective synthesis of (2*S*,3*S*,4*R*,5*S*)-5-methylpyrrolidine-3,4-diol derivatives that are highly selective α-L-fucosidase inhibitors, Chem. Commun. (2005) 4949–4951.
[31] P. Elías-Rodríguez, E. Moreno-Clavijo, A.T. Carmona, A.J. Moreno-Vargas, I. Robina, Rapid discovery of potent α-fucosidase inhibitors by *in situ* screening of a library of (pyrrolidin-2-yl)triazoles, Org. Biomol. Chem. 12 (2014) 5898–5904.
[32] A. Kotland, F. Accadbled, K. Robeyns, J.-B. Behr, Synthesis and fucosidase inhibitory study of unnatural pyrrolidine alkaloid 4-epi-(+)-codonopsinine, J. Org. Chem. 76 (2011) 4094–4098.
[33] C.-Y. Wu, C.-F. Chang, J.S.-Y. Chen, C.-H. Wong, C.-H. Lin, Rapid diversity-oriented synthesis in microtiter plates for *in situ* screening: discovery of potent and selective α-fucosidase inhibitors, Angew. Chem. Int. Ed. 42 (2003) 4661–4664.
[34] A. Hottin, D.W. Wright, G.J. Davies, J.-B. Behr, Exploiting the hydrophobic terrain in fucosidases with aryl-substituted pyrrolidine iminosugars, ChemBioChem 16 (2015) 277–283.
[35] X.-L. Qiu, F.-L. Qing, Synthesis of 3'-deoxy-3'-difluoromethyl azanucleosides from *trans*-4-hydroxy-L-proline, J. Org. Chem. 70 (2005) 3826–3837.
[36] H. Sarazin, S. Prudent, A. Defoin, C. Tarnus, Evaluation of 6-deoxy-amino-sugars as potent glycosidase inhibitors. importance of the $CH_2OH(6)$ group for enzyme-substrate interaction, ChemistrySelect 2 (2017) 1484–1490.
[37] E.-L. Tsou, Y.-T. Yeh, P.-H. Liang, W.-C. Cheng, A convenient approach toward the synthesis of enantiopure isomers of DMDP and ADMDP, Tetrahedron 65 (2009) 93–100.
[38] α-L-fucosidase (bovine kidney), α-glucosidase (*Saccharomyces cerevisiae* and rice), β-glucosidase (almonds), α-galactosidase (coffee beans), β-galactosidase (bovine liver), amyloglucosidase (*Aspergillus niger*), α-mannosidase (Jack beans), β-mannosidase (snail).
[39] V. Lombard, R.H. Golaconda, E. Drula, P.M. Coutinho, B. Henrissat, The carbohydrate-active enzymes database (CAZy) in 2013, Nucleic Acids Res. 42 (2014) D490–D495 [PMID: 24270786].
[40] R.L. Lieberman, B.A. Wustman, P. Huertas, A.C. Powe Jr., C.W. Pine, R. Khanna, M.G. Schlossmacher, D. Ringe, G.A. Petsko, Structure of acid beta-glucosidase with pharmacological chaperone provides insight into Gaucher disease, Nat. Chem. Biol. 3 (2007) 101–107.
[41] J. Zheng, L. Chen, O.S. Skinner, D. Ysselstein, J. Remis, P. Lansbury, R. Skerlj, M. Mrosek, U. Heunisch, S. Krapp, J. Charrow, M. Schwake, N.L. Kelleher, R.B. Silverman, D. Krainc, β-glucocerebrosidase modulators promote dimerization of β-glucocerebrosidase and reveal an allosteric binding site, J. Am. Chem. Soc. 140 (2018) 5914–5924.
[42] Z. Bikadi, E. Hazai, Application of the PM6 semi-empirical method to modeling proteins enhances docking accuracy of AutoDock, J. Cheminform. 1 (2009) 15.
[43] Y. Sun, B. Liou, Y.-H. Xu, B. Quinn, W. Zhang, R. Hamler, K.D.R. Setchell, G.A. Grabowski, Ex vivo and in vivo effects of isofagomine on acid β-glucosidase variants and substrate levels in Gaucher disease, J. Biol. Chem. 287 (2012) 4275–4287.
[44] T. Pirali, S. Gatti, R. Di Brisco, S. Tacchi, R. Zaninetti, E. Brunelli, A. Massarotti, G. Sorba, P.L. Canonico, L. Moro, A.A. Genazzani, G.C. Tron, R.A. Billington, Estrogenic analogues synthesized by click chemistry, ChemMedChem 2 (2007) 437–440.
[45] Z. Liu, J. Caner, A. Kudo, H. Naka, S. Saito, Redox-selective generation of aldehydes and H_2 from alcohols under visible light, Chem. Eur. J. 19 (2013) 9452–9456.
[46] S. Molchanov, W. Orzelski, A. Gryff-Keller, M.J. Potrzebowski, Magnetic shielding tensors of carbon nuclei in 3,5-dichlorophenylacetylene, a theoretical *ab initio* and experimental study, Mol. Phys. 100 (2002) 273–286.
[47] E. C. Constable, C. E. Housecroft, M. Neuburger, S. Reymann, S. Schaffner 4-Substituted and 4,5-disubstituted 3,6-di(2-pyridyl)pyridazines: ligands for supramolecular assemblies. Eur. J. Org. Chem., (2008), p. 1597–1607. For spectral properties, see: J. M. A. Robinson, B. M. Kariuki, K. D. M. Harris, D. Philp, Interchangeability of halogen and ethynyl substituents in the solid state structures of di- and tri-substituted benzenes. J. Chem. Soc., Perkin Trans. 2, (1998), p. 2459–2469.
[48] J.R. Suárez, B. Trastoy, M.E. Pérez-Ojeda, R. Marín-Barrios, J.L. Chiara, Octakis(3-azidopropyl)octasilsesquioxane: a versatile nanobuilding block for the efficient preparation of highly functionalized cube-octameric polyhedral oligosilsesquioxane frameworks through “click” assembly, Adv. Synth. Catal. 352 (2010) 2515–2520.
[49] H. Dvir, M. Harel, A.A. McCarthy, L. Toker, I. Silman, A.H. Futerman, J.L. Sussman, X-ray structure of human acid-beta-glucosidase, the defective enzyme in Gaucher disease, EMBO Rep. 4 (2003) 704–709.
[50] W. Kabsch, Software XDS for image rotation, recognition and crystal symmetry assignment, Acta Crystallogr. D Biol. Crystallogr. 66 (2010) 125–132.
[51] P. Emsley, B. Lohkamp, W.G. Scott, K. Cowtan, Features and development of Coot, Acta Crystallogr. D66 (2010) 486–501.
[52] T.A. Halgren, Merck molecular force field. I. Basis, form, scope, parametrization, and performance of MMFF94, J. Comp. Chem. 17 (1998) 490–519.
[53] G.M. Morris, D.S. Goodsell, R.S. Halliday, R. Huey, W.E. Hart, R.K. Belew, A.J. Olson, Automated docking using a Lamarckian genetic algorithm and an empirical binding free energy function, J. Comp. Chem. 19 (1999) 1639–1662.
[54] F.J. Solis, R.J.B. Wets, Minimization by random search techniques, Math. Op. Res. 6 (1981) 19–30.
[55] R.A. Laskowski, M.B. Swindells, LigPlot+: multiple ligand-protein interaction diagrams for drug discovery, J. Chem. Inf. Model. 51 (2011) 2778–2786.